

DO-TH 97/20

September 1997

revised February 1998

Dark matter constraints in the minimal and nonminimal SUSY standard model

A. Stephan

Universität Dortmund, Institut für Physik,
D-44221 Dortmund, Germany

Abstract

We determine the allowed parameter space and the particle spectra of the minimal SUSY standard model (MSSM) and nonminimal SUSY standard model (NMSSM) imposing correct electroweak gauge-symmetry breaking and recent experimental constraints. The parameters of the models are evolved with the SUSY RGEs assuming universality at the GUT scale. Applying the new unbounded from below (UFB) constraints we can exclude the LSP singlinos and light scalar and pseudoscalar Higgs singlets of the NMSSM. This exclusion removes the experimental possibility to distinguish between the MSSM and NMSSM via the recently proposed search for an additional cascade produced in the decay of the bino into the LSP singlino. Furthermore the effects of the dark matter condition for the MSSM and NMSSM are investigated and the differences concerning the parameter space, the SUSY particle and Higgs sector are discussed.

1 Introduction

If the standard model (SM) is embedded in a grand unified theory (GUT), finetuning is needed in order to have a Higgs mass of the order of the electroweak scale and not the GUT scale. The quadratic divergences in the radiative corrections to the Higgs mass are the reason for this naturalness problem in the SM. SUSY models have the advantage of being free of quadratic divergences due to cancellations in Feynman graphs with particles and their supersymmetric partners. The simplest SUSY extension of the SM is the minimal SUSY standard model (MSSM) [1, 2] with two Higgs doublets H_1 and H_2 . However the MSSM has also a naturalness problem why the μ -parameter of the term $\mu H_1 H_2$ in the superpotential should be much smaller than the Planck mass. The nonminimal SUSY standard model (NMSSM) [3] is a minimal extension of the MSSM. In this model a Higgs singlet N is added to the Higgs sector of the MSSM. Moreover the μ -parameter of the MSSM can be dynamically generated via $\mu = \lambda x$ with the term $\lambda H_1 H_2 N$ in the superpotential of the NMSSM, if the Higgs singlet acquires a vacuum expectation value (VEV) $\langle N \rangle = x$. SUSY models with Higgs singlets can be derived from superstring inspired E_6 or $SU(5) \times U(1)$ GUT models and they offer the possibility of spontaneous breaking of the CP symmetry. The discrete \mathbb{Z}_3 symmetry of the NMSSM causes a domain wall problem. In the early universe the \mathbb{Z}_3 symmetry is spontaneously broken during the electroweak phase transition. Domains of different degenerate vacua develop which are separated by domain walls. Since these domain walls would dominate the energy density of the universe and disturb primordial nucleosynthesis, they have to disappear before the onset of nucleosynthesis. Possible solutions to the domain wall problem and the hierarchy problem reintroduce the terms $\mu H_1 H_2$ and $\mu' N^2$ in the superpotential of the NMSSM and possess a gauged R-symmetry or a target space duality symmetry at the Planck scale [4]. In these more general models the NMSSM is approximated for very small values of the parameters μ and μ' .

The addition of a Higgs singlet superfield leads to two extra Higgses and one extra neutralino in the NMSSM compared to the particle spectrum of the MSSM. Since the Higgs singlets and the singlino \tilde{N} can mix with the other Higgses and neutralinos, the phe-

nomenology of the NMSSM may be modified compared to the MSSM. The phenomenology of the NMSSM has been investigated in several papers [5] - [15]. In SUSY models with R-parity conservation the lightest SUSY particle (LSP) cannot decay and is therefore stable. Especially a neutral LSP like the lightest neutralino is a good candidate for cold dark matter. In the MSSM the dark matter neutralino is mostly a bino. In the NMSSM there exists the alternative of a dark matter neutralino with a larger singlino portion. The cosmology of these dark matter singlinos has been discussed in [16] at a given fixed low energy scale. The experimentally and cosmologically allowed parameter space of the NMSSM and the dark matter neutralinos have been investigated in [17] using SUSY RG evolutions.

In the present paper we compare the allowed parameter space and the particle spectra of the MSSM and NMSSM. Assuming universality at the GUT scale the parameters of the models are evolved to the electroweak scale with the SUSY RGEs (given in [18] and Appendix A2 for the NMSSM). The Higgs potential is minimized and additional theoretical constraints and recent experimental bounds are imposed. Besides charge and color breaking (CCB) constraints we include here new unbounded from below (UFB) constraints [19]. Furthermore the consequences of the dark matter condition for the MSSM and NMSSM are investigated. In the present paper we give a more detailed analysis of the two models and the dark matter condition than in our previous paper [20].

In section 2 we introduce the NMSSM. The additional theoretical and experimental constraints are discussed in section 3. In section 4 we describe the dark matter constraints. The procedure of finding solutions of the NMSSM is explained in section 5. In section 6 the parameter space and the particle spectra of the MSSM and NMSSM are investigated without and with the dark matter condition. In Appendix A1 we give the complete formulas for the neutralino annihilation cross section in the NMSSM which are needed to calculate the relic neutralino density. In Appendix A2 the SUSY RGEs [18] for the NMSSM are listed.

2 The NMSSM

The Higgs sector of the MSSM consists of two Higgs doublets H_1 and H_2 . In the NMSSM [3] an additional Higgs singlet N is introduced. The superpotential of the NMSSM contains only Yukawa terms with dimensionless couplings

$$W = h_d H_1^T \epsilon \tilde{Q} \tilde{D} - h_u H_2^T \epsilon \tilde{Q} \tilde{U} + \lambda H_1^T \epsilon H_2 N - \frac{1}{3} k N^3. \quad (1)$$

\tilde{Q} is a squark doublet. \tilde{U} and \tilde{D} are up-type and down-type squark singlets. ϵ is the antisymmetric tensor with $\epsilon_{12} = 1$. The SUSY breaking is parametrized by different types of SUSY soft breaking terms in the lagrangian:

$$\begin{aligned} \mathcal{L}_{soft} = & -m_{H_1}^2 |H_1|^2 - m_{H_2}^2 |H_2|^2 - m_N^2 |N|^2 - m_Q^2 |\tilde{Q}|^2 - m_U^2 |\tilde{U}|^2 - m_D^2 |\tilde{D}|^2 \\ & - h_d A_d H_1^T \epsilon \tilde{Q} \tilde{D} + h_u A_u H_2^T \epsilon \tilde{Q} \tilde{U} \\ & + \lambda A_\lambda H_1^T \epsilon H_2 N + \frac{1}{3} k A_k N^3 \\ & + \frac{1}{2} M_3 \lambda_3 \lambda_3 + \frac{1}{2} M_2 \lambda_2^a \lambda_2^a + \frac{1}{2} M_1 \lambda_1 \lambda_1 + h.c. \end{aligned} \quad (2)$$

In SUSY models the tree-level scalar potential is given by the formula:

$$V_{tree} = \frac{1}{2} \sum (D^a)^2 + \sum F_i^* F_i + V_{soft} \quad (3)$$

$$D^a = g_a A_i^* T_{ij}^a A_j, \quad (4)$$

$$F_i = - \left(\frac{\partial W}{\partial A_i} \right)^* \quad (5)$$

where A_i are scalar fields and T_{ij}^a are the gauge group generators. The part of the scalar potential with only Higgs fields corresponds to the Higgs potential. The neutral part of the tree-level Higgs potential is given by:

$$\begin{aligned} V_{tree}^{Higgs} = & m_{H_1}^2 |H_1^0|^2 + m_{H_2}^2 |H_2^0|^2 + m_N^2 |N|^2 + \lambda^2 (|H_1^0|^2 + |H_2^0|^2) |N|^2 + \lambda^2 |H_1^0|^2 |H_2^0|^2 \\ & + k^2 |N|^4 - \lambda k H_1^0 H_2^0 N^{*2} - \lambda A_\lambda H_1^0 H_2^0 N - \frac{1}{3} k A_k N^3 \\ & + \frac{1}{8} (g_y^2 + g_2^2) (|H_1^0|^2 - |H_2^0|^2)^2 + h.c. \end{aligned} \quad (6)$$

In order to calculate the Higgs VEVs reliably we use the effective 1 loop Higgs potential consisting of the tree-level Higgs potential and the radiative corrections

$$V_{1loop}^{Higgs} = V_{tree}^{Higgs} + V_{rad}^{Higgs}. \quad (7)$$

The radiative corrections [6] to the effective Higgs potential arising from all particles and antiparticles with field-dependent mass m_i , spin S_i and color degrees of freedom C_i are given by

$$V_{rad}^{Higgs} = \frac{1}{64 \pi^2} \sum_i C_i (-1)^{2S_i} (2S_i + 1) m_i^4 \ln\left(\frac{m_i^2}{Q^2}\right). \quad (8)$$

Q is the renormalisation scale which we take to be equal to the electroweak scale $M_{weak} \simeq 100 \text{ GeV}$. Here we only consider the important contributions of the top quark and stops $\tilde{t}_{1,2}$. The electroweak gauge-symmetry $SU(2)_I \times U(1)_Y$ is spontaneously broken to the electromagnetic gauge-symmetry $U(1)_{em}$ by the Higgs VEVs $\langle H_i^0 \rangle = v_i$ with $i = 1, 2$ and $\langle N \rangle = x$. The local minimum of the effective 1 loop Higgs potential is determined by the three minimum conditions for the VEVs:

$$\frac{1}{2} m_Z^2 = \frac{m_{H_1}^2 + \Sigma^1 - (m_{H_2}^2 + \Sigma^2) \tan^2 \beta}{\tan^2 \beta - 1} - \lambda^2 x^2 \quad (9)$$

$$\sin(2\beta) = \frac{2 \lambda x (A_\lambda + k x)}{m_{H_1}^2 + \Sigma^1 + m_{H_2}^2 + \Sigma^2 + 2 \lambda^2 x^2 + \lambda^2 v^2} \quad (10)$$

$$(m_N^2 + \Sigma^3) x^2 - k A_k x^3 + 2 k^2 x^4 + \lambda^2 x^2 v^2 - \frac{1}{2} (A_\lambda + 2 k x) \lambda x v^2 \sin(2\beta) = 0 \quad (11)$$

where $v = \sqrt{v_1^2 + v_2^2} = 174 \text{ GeV}$, $\tan \beta = v_2/v_1$ and $\Sigma^i = \partial V_{rad}^{Higgs} / \partial v_i^2$.

The neutralinos are Majorana particles and mixed states of the gauginos and Higgsinos. The mass and composition of the neutralinos is defined by the following part of the lagrangian

$$\mathcal{L} = -\frac{1}{2} \Psi^T M \Psi + h.c. \quad (12)$$

$$\Psi^T = (-i\lambda_1, -i\lambda_2^3, \Psi_{H_1}^0, \Psi_{H_2}^0, \Psi_N). \quad (13)$$

In this basis the symmetric mass matrix M of the neutralinos has the form:

$$\left(\begin{array}{ccccc} M_1 & 0 & -m_Z \sin \theta_W \cos \beta & m_Z \sin \theta_W \sin \beta & 0 \\ 0 & M_2 & m_Z \cos \theta_W \cos \beta & -m_Z \cos \theta_W \sin \beta & 0 \\ -m_Z \sin \theta_W \cos \beta & m_Z \cos \theta_W \cos \beta & 0 & \lambda x & \lambda v_2 \\ m_Z \sin \theta_W \sin \beta & -m_Z \cos \theta_W \sin \beta & \lambda x & 0 & \lambda v_1 \\ 0 & 0 & \lambda v_2 & \lambda v_1 & -2 k x \end{array} \right).$$

With $\mu = \lambda x$ the first 4×4 submatrix recovers the mass matrix of the MSSM [2]. The mass of the neutralinos is here obtained by diagonalising the mass matrix M with the orthogonal matrix N . (Then some mass eigenvalues may be negative [21].)

$$\mathcal{L} = -\frac{1}{2} m_i \tilde{\chi}_i^0 \tilde{\chi}_i^0 \quad (14)$$

$$\tilde{\chi}_i^0 = \begin{pmatrix} \chi_i^0 \\ \bar{\chi}_i^0 \end{pmatrix} \text{ with } \chi_i^0 = N_{ij} \Psi_j \text{ and } M_{diag} = N M N^T. \quad (15)$$

The neutralinos $\tilde{\chi}_i^0$ ($i = 1 - 5$) are ordered with increasing mass $|m_i|$, thus $\tilde{\chi}_1^0$ is the LSP neutralino. The matrix elements N_{ij} ($i, j = 1 - 5$) describe the composition of the neutralino $\tilde{\chi}_i^0$ in the basis Ψ_j (Eq.(13)). For example the bino portion of the LSP neutralino is given by N_{11}^2 and the singlino portion of the LSP neutralino by N_{15}^2 . The diagonalising of the mass matrix M leads to a polynomial equation of degree 5, which cannot be solved analytically in general. Therefore we calculate the eigenvalues and eigenvectors of the symmetric mass matrix M numerically by using a subroutine in the NAG Fortran Library.

The possibility of gauge coupling unification is an important motivation for SUSY GUTs. In contrast to non-supersymmetric GUTs [22], the gauge couplings in SUSY GUTs are allowed to unify $g_a(M_X) = g_5 \simeq 0.72$ at a scale $M_X \simeq 1.6 \times 10^{16} \text{ GeV}$. Within a minimal $N = 1$ supergravity framework universality naturally arises for the SUSY soft breaking parameters:

$$\begin{aligned} m_i(M_X) &= m_0 \\ M_a(M_X) &= m_{1/2} \\ A_i(M_X) &= A_0 \quad (A_\lambda(M_X) = -A_0). \end{aligned} \quad (16)$$

The Yukawa couplings at the GUT scale take the values $\lambda(M_X) = \lambda_0$, $k(M_X) = k_0$ and $h_t(M_X) = h_{t0}$. With the SUSY RGEs ([18], Appendix A2) the SUSY soft breaking parameters and the Yukawa couplings are evolved from the GUT scale to the electroweak scale M_{weak} . At M_{weak} we minimize the effective 1 loop Higgs potential V_{1loop}^{Higgs} (Eq.(7)).

3 Theoretical and experimental constraints

The solutions of the SUSY RGEs ([18], Appendix A2) have to fulfill several theoretical and experimental constraints. The minimum of the effective 1 loop Higgs potential V_{1loop}^{Higgs}

(Eq.(7)) should be not only a local minimum but also a stable minimum. A local minimum is stable against tunnelling into a lower minimum, if its lifetime is large enough (of the order of the age of the universe). A global minimum is certainly stable, but it may be difficult to prove, that it is really a global minimum. Here we only investigate, whether the physical minimum is lower than the unphysical minima of $V_{loop}^{Higgs}(v_1, v_2, x)$ with at least one vanishing VEV [5].

The conservation of charge and color would be broken by slepton and squark VEVs. To avoid a scalar potential with such a minimum, the trilinear couplings have to fulfill the following conditions [18]:

$$A_{u_i}^2 \leq 3(m_{H_2}^2 + m_{Q_i}^2 + m_{U_i}^2) \text{ at scale } Q \sim A_{u_i}/h_{u_i} \quad (17)$$

$$A_{d_i}^2 \leq 3(m_{H_1}^2 + m_{Q_i}^2 + m_{D_i}^2) \text{ at scale } Q \sim A_{d_i}/h_{d_i} \quad (18)$$

$$A_{e_i}^2 \leq 3(m_{H_1}^2 + m_{L_i}^2 + m_{E_i}^2) \text{ at scale } Q \sim A_{e_i}/h_{e_i}. \quad (19)$$

In [19] improved charge and color breaking (CCB) constraints and unbounded from below (UFB) constraints are analysed for the MSSM. The by far strongest of these new constraints is the UFB-3 constraint (Eq.(33) in the first publication of Ref.[19]), in contrast to the remaining ones. To apply the UFB-3 constraint to the NMSSM we have to modify the formulas in [19]: In the NMSSM a dangerous field direction of the tree-level scalar potential V_{tree} (Eq.(3)) occurs for VEVs of the neutral Higgs H_2^0 , the electron sneutrino $\tilde{\nu}_e$ denoted by $L_1 = \tilde{L}_1^0$ and the staus $\tilde{\tau}_L^-$ and $\tilde{\tau}_R^+$ denoted by \tilde{L}_3^- and \tilde{E}_3 . The VEVs of the staus are introduced in order to cancel the F-term of H_1^0 :

$$\left| \frac{\partial W}{\partial H_1^0} \right|^2 = | \lambda x H_2^0 + h_\tau \tilde{L}_3^- \tilde{E}_3 |^2 = 0. \quad (20)$$

For the VEVs of the staus we choose the relation $e = \tilde{L}_3^- = \tilde{E}_3$. In analogy to the MSSM we have replaced in Eq.(20) μ by λx where the Higgs singlet VEV $\langle N \rangle = x$ is determined by the physical minimum of the NMSSM Higgs potential. Since we consider here the scalar potential and not only the Higgs potential, the Higgs singlet VEV x may be optimized further. But here we don't investigate this more general case. The NMSSM tree-level scalar potential along the described field direction is given by:

$$V_{tree} = m_{H_2}^2 |H_2^0|^2 + (m_{L_3}^2 + m_{E_3}^2) |e|^2 + m_{L_1}^2 |L_1|^2$$

$$\begin{aligned}
& + \frac{1}{8} (g_y^2 + g_2^2) (|H_2^0|^2 + |e|^2 - |L_1|^2)^2 \\
& + m_N^2 x^2 - \frac{2}{3} k A_k x^3 + k^2 x^4.
\end{aligned} \tag{21}$$

Now we can determine the dangerous field direction of V_{tree} (Eq.(21)), which is given by:

$$|L_1|^2 = \frac{-4 m_{L_1}^2}{g_y^2 + g_2^2} + |H_2^0|^2 + |e|^2, \tag{22}$$

$$|e| = \sqrt{\frac{|\lambda x|}{h_\tau} |H_2^0|} \tag{23}$$

provided that

$$|H_2^0| > \sqrt{\frac{(\lambda x)^2}{4 h_\tau^2} + \frac{4 m_{L_1}^2}{g_y^2 + g_2^2}} - \frac{\lambda x}{2 h_\tau}. \tag{24}$$

For smaller values of $|H_2^0|$ we obtain $|L_1| = 0$. In the field direction of Eq.(22) and (23) the tree-level scalar potential of the NMSSM reads:

$$\begin{aligned}
V_{UFB-3} & = (m_{H_2}^2 + m_{L_1}^2) |H_2^0|^2 + \frac{|\lambda x|}{h_\tau} (m_{L_3}^2 + m_{E_3}^2 + m_{L_1}^2) |H_2^0| \\
& - \frac{2 m_{L_1}^4}{g_y^2 + g_2^2} + m_N^2 x^2 - \frac{2}{3} k A_k x^3 + k^2 x^4.
\end{aligned} \tag{25}$$

For $|L_1| = 0$ the tree-level scalar potential is given by:

$$\begin{aligned}
V_{UFB-3} & = m_{H_2}^2 |H_2^0|^2 + \frac{|\lambda x|}{h_\tau} (m_{L_3}^2 + m_{E_3}^2) |H_2^0| \\
& + \frac{1}{8} (g_y^2 + g_2^2) \left(|H_2^0|^2 + \frac{|\lambda x|}{h_\tau} |H_2^0| \right)^2 + m_N^2 x^2 - \frac{2}{3} k A_k x^3 + k^2 x^4.
\end{aligned} \tag{26}$$

Since the tree-level scalar potential V_{UFB-3} should be larger than the physical minimum of the tree-level Higgs potential V_{tree}^{Higgs} (Eq.(6)), the UFB-3 constraint can be written as

$$V_{UFB-3}(Q = \hat{Q}) > (V_{tree}^{Higgs}(Q = M_S))_{Min}. \tag{27}$$

The tree-level Higgs potential V_{tree}^{Higgs} (Eq.(6)) is minimized at the scale $Q = M_S$, where the radiative corrections V_{rad}^{Higgs} (Eq.(8)) are very small. M_S turns out to be a certain average of SUSY masses. For the same reason the tree-level scalar potential V_{UFB-3} is evaluated at the scale $Q = \hat{Q} \sim Max(g_2 |e|, g_2 |H_2^0|, h_t |H_2^0|, g_2 |L_1|, M_S)$. Since $V_{UFB-3}(Q = \hat{Q})$ depends on $|H_2^0|$ the relation (27) should be fulfilled for all $|H_2^0|$ values below M_X .

Because we assume $h_t \gg h_b, h_\tau$, we restrict $|\tan\beta|$ to be smaller than 20 [7]. For the Higgs singlet VEV x we choose the range $|x| < 80 \text{ TeV}$ [7, 8, 13]. In the present paper we choose the parameters m_0 and $|m_{1/2}|$ to be smaller than 1500 GeV . This restriction is motivated by requiring the absence of too much fine-tuning [13], which disfavors solutions with enormous sensitivity of m_Z to the GUT scale parameters h_{t0} or λ_0 and k_0 . The dark matter constraints further restrict the allowed parameter region of m_0 and $|m_{1/2}|$ as shown in Fig.1.

For the top quark pole mass we take the range $169 \text{ GeV} < m_t < 181 \text{ GeV}$ corresponding to the recent world average measurement [23]. Since charged or colored massive stable particles are cosmologically disfavored LSPs, we assume the lightest neutralino to be the LSP and impose the constraints $m_{\tilde{\chi}_1^0} < m_{\tilde{\tau}_1}$ and $m_{\tilde{\chi}_1^0} < m_{\tilde{t}_1}$. The SUSY particles in the NMSSM have to fulfill the following experimental conditions: $m_{\tilde{\nu}} \geq 41.8 \text{ GeV}$ [24], $m_{\tilde{e}_R} \geq 70 \text{ GeV}$ [25], $m_{\tilde{q}} \geq 176 \text{ GeV}$ (if $m_{\tilde{g}} < 300 \text{ GeV}$) [24] and $m_{\tilde{q}} \geq 70 \text{ GeV}$ (for all $m_{\tilde{g}}$) [26], $m_{\tilde{t}_1} \geq 63 \text{ GeV}$ [25], $m_{\tilde{g}} \geq 173 \text{ GeV}$ [27], $m_{\tilde{\chi}_1^+} \geq 85.4 \text{ GeV}$ [28], $m_{H^+} \geq 52 \text{ GeV}$ [29], $m_{S_1} \geq 74 \text{ GeV}$ [30] or the coupling of the lightest scalar Higgs S_1 to the Z boson is reduced compared to the SM [31] assuming visible decays with branching ratios like the SM Higgs [8], and

$$\sum_{i,j} \Gamma(Z \rightarrow \tilde{\chi}_i^0 \tilde{\chi}_j^0) < 30 \text{ MeV} \quad [32]$$

$$\Gamma(Z \rightarrow \tilde{\chi}_1^0 \tilde{\chi}_1^0) < 7 \text{ MeV} \quad [32]$$

$$BR(Z \rightarrow \tilde{\chi}_i^0 \tilde{\chi}_j^0) < 10^{-5}, \quad (i,j) \neq (1,1) \quad [32].$$

4 Dark matter constraints

Inflationary cosmological models are proposed to solve the flatness, horizon and magnetic monopole problem. In these models the universe is flat with a density equal to the critical density $\rho_{crit} = 1.054 \times 10^{-5} h_0^2 \text{ GeV}/\text{cm}^3$ implying a cosmological density parameter of $\Omega = \rho/\rho_{crit} = 1$. The Hubble constant $H_0 = 100 h_0 \text{ km s}^{-1} \text{ Mpc}^{-1}$ is restricted by observations to the range $0.4 < h_0 < 1$ of the scaled Hubble constant h_0 . To be consistent with the observed abundances of the isotopes D , ${}^3\text{He}$, ${}^4\text{He}$ and ${}^7\text{Li}$ the big bang

nucleosynthesis model restricts the baryon density to $\Omega_{baryons} \leq 0.1$. The discrepancy between the cosmological density $\Omega = \rho/\rho_{crit} = 1$ and the baryon density requires a huge amount of dark matter in the universe. One of the favored theories to explain the structure formation of the universe is the cold + hot dark matter model (CHDM) [33]. In this model the dark matter consists of hot dark matter (massiv neutrinos) and cold dark matter (neutralinos) with $\Omega_{hot} \simeq 0.3$ and $\Omega_{cold} \simeq 0.65$. With the allowed range of the scaled Hubble constant h_0 the condition for the relic density of the neutralinos in the CHDM model reads

$$0.1 \leq \Omega_\chi h_0^2 \leq 0.65. \quad (28)$$

The relic neutralino density can be calculated by solving the Boltzmann equation for the early universe. The Boltzmann equation describes the particle densities in the cosmic plasma governed by the annihilation cross section. The annihilation cross section of the neutralinos can be expanded in powers of the relative velocity v of the non-relativistic neutralinos: $\sigma_{ann}v = a + bv^2$. The thermally averaged annihilation cross section [34] - [36] is then given by $\langle \sigma_{ann}v \rangle = x^{1.5} / (2\sqrt{\pi}) \int_0^\infty dv v^2 \exp\{-x v^2 / 4\} \sigma_{ann}v = a + 6b/x$ with $x = |m_{\tilde{\chi}_1^0}| / T$. During the expansion of the universe its temperature falls and reaches the freeze-out temperature of the neutralinos T_{fr} , at which the neutralinos drop out of the thermal equilibrium with the cosmic plasma. The freeze-out temperature of the neutralinos T_{fr} follows from the equation [34] - [37]

$$x_{fr} = \ln \left(0.0764 |m_{\tilde{\chi}_1^0}| M_P \frac{\langle \sigma_{ann}v \rangle}{\sqrt{g_*} x_{fr}} c (2 + c) \right), \quad (29)$$

where $M_P = 1.221 \times 10^{19} GeV$ is the Planck mass, $g_* \approx 81$ is the effective number of degrees of freedom at T_{fr} and $c = 1/2$. With $J(x_{fr}) = \int_{x_{fr}}^\infty dx/x^2 \langle \sigma_{ann}v \rangle = a/x_{fr} + 3b/x_{fr}^2$ [34] - [36] the relic neutralino density [34] - [37] is given by

$$\Omega_\chi h_0^2 = \frac{1.07 \times 10^9}{\sqrt{g_*} M_P J(x_{fr}) GeV}. \quad (30)$$

The expansion of the annihilation cross section $\sigma_{ann}v = a + bv^2$ is not a good approximation in the vicinity of poles or thresholds [38]. In the present work the case of coannihilation is not important [17, 39], since the LSP neutralino in the MSSM and NMSSM is mostly bino-like or a mixed state with small mass (see Fig.4). Furthermore the LSP singlinos

[9, 10, 13] of the NMSSM are now excluded by the UFB-3 constraint (Eq.(27)) as discussed in section 6.

Compared to the MSSM the annihilation cross section of the neutralinos changes in the NMSSM because of more particles in this model, which can mix, and modified vertices. In our numerical analysis we consider all possible decay channels. The relevant formulas for the NMSSM are given in the Appendix A1. They are obtained by substituting the MSSM couplings in [34] by the corresponding NMSSM couplings and by slightly modifying the partial wave amplitudes in [34].

5 Procedure of finding solutions

The SUSY soft breaking parameters m_i and A_i and the Yukawa couplings λ , k and h_t are evolved with the SUSY RGEs ([18], Appendix A2) from the GUT scale M_X to the electroweak scale M_{weak} . Since we assume universality at the GUT scale M_X (Eq.(16)) we have only 6 GUT scale parameters m_0 , $m_{1/2}$, A_0 , λ_0 , k_0 and h_{t0} . Together with the low energy parameters $\tan \beta$ and x there are 8 parameters in the NMSSM with only 5 of them being independent. In our procedure we take λ_0 , k_0 , h_{t0} , $\tan \beta$ and x as independent input parameters. The remaining 3 parameters (m_0 , $m_{1/2}$, A_0) are then determined by the three minimum conditions (9-11) and are numerically calculated by the method described in [7, 20]: The three minimum conditions (9-11) depend only on the low energy parameters m_i , A_i , λ , k and h_t generically denoted by $p_k(M_{weak})$:

$$\frac{\partial V_{1loop}}{\partial v_i} = F_i(p_k) = 0 \quad (i = 1 - 3). \quad (31)$$

Since λ_0 , k_0 and h_{t0} are (randomly chosen) fixed input parameters, all low energy parameters $p_k(M_{weak})$ are functions f_k (which can be constant) of the GUT scale parameters m_0 , $m_{1/2}$ and A_0 only:

$$p_k(M_{weak}) = f_k(m_0, m_{1/2}, A_0). \quad (32)$$

To obtain the functions f_k we numerically solve the SUSY RGEs ([18], Appendix A2) $dp_k/dt = h_k(t, p_1, \dots, p_n)$ ($k = 1 - n$). A solution to a system of first-order differential

equations can be found with the method of Runge, Kutta and Merson. A subroutine for this numerical method is available in the CERN Program Library. An additional subroutine has to be written which calculates the derivatives dp_k/dt ($k = 1 - n$) depending on the current values of t and p_1, \dots, p_n . In the three minimum conditions (31) we then substitute the low energy parameters $p_k(M_{weak})$ by the functions f_k and obtain the generic equations

$$F_i(f_k(m_0, m_{1/2}, A_0)) = G_i(m_0, m_{1/2}, A_0) = 0 \quad (i = 1 - 3). \quad (33)$$

The SUSY breaking parameters m_0 , $m_{1/2}$ and A_0 are then determined by the zero points of the generic equations $G_i(m_0, m_{1/2}, A_0) = 0$ ($i = 1 - 3$). In order to find a solution of Eq.(33) we first minimize $\sum_{i=1}^3 G_i(m_0, m_{1/2}, A_0)^2$ and then we check, whether the minimum is also a zero point. The minimization is performed by using the simplex method of Nelder and Mead. A corresponding minimization routine SIMPLEX is available in the MINUIT package of the CERN Program Library. The numerical procedure needs starting values for the parameters m_0 , $m_{1/2}$ and A_0 , which are randomly generated using a logarithmic measure within their ranges.

To obtain a representative sample of solutions of the NMSSM, we randomly generate $\sim 4.3 \times 10^8$ points in the 5 dimensional parameter space of the input parameters λ_0 , k_0 , h_{t0} , $\tan \beta$ and x using a logarithmic measure. The SUSY breaking parameters m_0 , $m_{1/2}$ and A_0 are then numerically calculated with the three minimum equations (33). Having found a solution of the SUSY RGEs ([18], Appendix A2), whose effective 1 loop Higgs potential V_{1loop}^{Higgs} (Eq.(7)) has a local minimum for the input parameters $\tan \beta$ and x , we impose the additional theoretical and experimental constraints described in section 3. The very strong UFB-3 constraint (Eq.(27)) excludes about 80% of the solutions which fulfill all the other constraints of section 3. For every solution we calculate the masses of all SUSY particles [2, 40] and Higgses [3, 6, 12, 13]. Altogether we obtain about 6600 solutions which fulfill all requirements. The ranges of the parameters, for which we find solutions, are given by $m_0 \in [60 \text{ GeV}, 1500 \text{ GeV}]$, $|m_{1/2}| \in [120 \text{ GeV}, 1500 \text{ GeV}]$, $|A_0| \in [180 \text{ GeV}, 6000 \text{ GeV}]$, $\lambda_0 \in [2 \times 10^{-3}, 0.5]$, $k_0 \in [10^{-3}, 0.6]$, $h_{t0} \in [0.4, 0.9]$, $|\tan \beta| \in [2.4, 20]$ and $|x| \in [800 \text{ GeV}, 80000 \text{ GeV}]$. Applying the dark matter constraint to the 6600 solutions, about 1500 solutions remain which are cosmologically

acceptable.

6 Parameter space and particle spectra

In the following we investigate the parameter space and the particle spectra of the MSSM and NMSSM. The consequences of the dark matter condition for the two models are discussed. We show our results in the form of scatter-plots. Each point represents a solution of the SUSY RGEs (given in Appendix A2 for the NMSSM) with additional theoretical and experimental constraints imposed as described for the NMSSM in section 3. In the upper left picture of Fig.1 the MSSM solutions are shown in the $(|m_{1/2}|, m_0)$ plane. The parameter region with small m_0 and large $|m_{1/2}|$ is excluded by the UFB-3 constraint [19]. Furthermore in the region $|m_{1/2}| \gg m_0$ the stau or stop would be the LSP. But a charged or colored LSP like the stau or stop is cosmologically disfavored [41]. In the upper right picture the cosmologically allowed solutions are shown. The dark matter condition leads to an upper bound of 600 GeV for $|m_{1/2}|$ and leaves m_0 unconstrained. Values of m_0 larger than about 300 GeV are cosmologically allowed due to Z-pole or Higgs-pole enhanced neutralino pair annihilation. Comparable scatter-plots for the constrained MSSM are discussed in [42]. In that paper upper bounds of 940 GeV for $|m_{1/2}|$ and 500 GeV for m_0 are deduced for $m_t = 170 \text{ GeV}$. The lower left picture shows the NMSSM solutions. The effect of the UFB-3 constraint (Eq.(27)) in the NMSSM is comparable to the MSSM. In the NMSSM this constraint also excludes the parameter region with small m_0 and large $|m_{1/2}|$. The reason, why the case $m_0 \gg |m_{1/2}|$ is suppressed in the NMSSM, is discussed in [9]. It follows from the condition, that the minimum of the scalar potential does not break the conservation of charge and color, and from the condition that the physical minimum is lower than the symmetric vacuum, $9 m_0^2 \lesssim A_0^2$. In the lower right picture the dark matter condition is imposed leading to an upper bound of 650 GeV for $|m_{1/2}|$. In contrast to the MSSM the upper bound for m_0 is about 300 GeV in the NMSSM. These upper bounds follow from the cosmological upper bounds of 260 GeV for the LSP neutralino and 450 GeV for the lighter selectron as discussed in [20] and below. This can be understood from the fact [34], that the LSP neutralino in the NMSSM is mostly bino-like (see Fig.4)

and the annihilation cross section is dominated by sfermion exchange.

For the MSSM we show in the upper left picture of Fig.2 the solution points in the plane $(m_0, |A_0|)$. The upper bound for $|A_0|$ follows from the UFB-3 constraint [19]. The upper right picture shows the cosmologically restricted solutions. The concentration of points corresponds to m_0 values below about $300 GeV$ in the upper right picture of Fig.1. Larger values of m_0 are cosmologically allowed because of Z-pole or Higgs-pole enhanced neutralino pair annihilation. The lower left picture shows the allowed values of $|A_0|$ in the NMSSM. Comparable with the MSSM the UFB-3 constraint (Eq.(27)) leads to an upper bound for $|A_0|$ in the NMSSM. In contrast to the MSSM there is also a lower bound for $|A_0|$ in the NMSSM. The NMSSM solutions have to fulfill the relation $9 m_0^2 \lesssim A_0^2$ [9], which follows from the condition that the physical minimum has to be lower than the symmetric vacuum. The dark matter condition strongly restricts the allowed range of $|A_0|$ as shown in the lower right picture. Larger values of m_0 are cosmologically excluded, since $m_0 \gg |m_{1/2}|$ is disfavored in the NMSSM as already discussed.

In the upper left picture of Fig.3 we show the MSSM solution points in the plane $(\mu, |M_2|)$. The parameters μ and M_2 are taken at the electroweak scale M_{weak} . The solutions are lying below the diagonals $|M_2| = |\mu|$. The reason is the first minimum condition which favors larger values of $|\mu|$ for $|\tan \beta| \rightarrow 1$. The first minimum condition of the MSSM has the same form as the first minimum condition in the NMSSM (Eq.(9)) if μ is substituted for λx . This property of the solutions leads to bino-like LSP neutralinos in the MSSM (see Fig.4). In the upper right picture the dark matter condition is imposed. The upper bound of $500 GeV$ for $|M_2|$ corresponds to the upper bound of $600 GeV$ for $|m_{1/2}|$ in the upper right picture of Fig.1. The NMSSM solutions in the lower left picture are similar to the MSSM solutions, but they are more restricted. This restriction follows from the third minimum condition (Eq.(11)) in the NMSSM which would be an extra constraint for the MSSM. The lower right picture shows the cosmologically allowed solutions. The upper bound of $550 GeV$ for $|M_2|$ follows from the upper bound of $650 GeV$ for $|m_{1/2}|$ in the lower right picture of Fig.1.

In the upper left picture of Fig.4 the bino portion of the LSP neutralino $|\langle \tilde{B} | \tilde{\chi}_1^0 \rangle|^2$

versus the LSP neutralino mass is shown for the MSSM. The LSP neutralinos are mostly binos $|\langle \tilde{B} | \tilde{\chi}_1^0 \rangle|^2 \approx 1$, which follows from the first minimum condition in the MSSM corresponding to Eq.(9) as already discussed. The cosmologically allowed LSP neutralinos are shown in the upper right picture. The dark matter condition sets an upper bound of 240 GeV for the LSP neutralino mass corresponding to the upper bound of 600 GeV for $|m_{1/2}|$ in the upper right picture of Fig.1. The lower bound for the mass of the LSP neutralinos is about 40 GeV in the MSSM. For the NMSSM the lower left picture shows the bino portion of the LSP neutralinos. Similarly to the MSSM most of the LSP neutralinos are binos in the NMSSM. If the UFB-3 constraint (Eq.(27)) is not applied, there exist a large fraction of decoupled pure LSP singlinos with $|\langle \tilde{B} | \tilde{\chi}_1^0 \rangle|^2 = 0$ and a much smaller fraction of mixed LSP singlinos. In [10] the phenomenology of the LSP singlinos is investigated. The LSP singlinos are now excluded by the UFB-3 constraint (Eq.(27)), which excludes the parameter region with small m_0 and large $|m_{1/2}|$. This is just the appropriate parameter region for LSP singlinos [9, 10, 13]. The lower right picture shows the cosmologically allowed LSP neutralinos in the NMSSM. The upper bound of 260 GeV for the LSP neutralino mass corresponds to the upper bound of 650 GeV for $|m_{1/2}|$ in the lower right picture of Fig.1. The dark matter condition improves the lower bound for the LSP neutralinos in the NMSSM to 50 GeV as discussed in [20]. In the NMSSM all LSP neutralinos with mass $m_{\tilde{\chi}_1^0} \approx m_Z/2$ are cosmologically excluded, since their coupling to the Z boson is larger due to a larger Higgsino portion.

In the upper left picture of Fig.5 the mass of the lighter chargino versus the mass of the lighter selectron is shown for the MSSM. The upper right picture shows the cosmologically allowed lighter chargino masses. The dark matter condition sets an upper bound of 450 GeV for the lighter chargino and disfavors somewhat selectron masses larger than about 1 TeV . Selectrons with $300 \text{ GeV} \lesssim m_{\tilde{e}_R}$ are cosmologically allowed due to Z-pole or Higgs-pole enhanced neutralino pair annihilation [42]. For the NMSSM the lower left picture shows the mass of the lighter chargino versus the mass of the lighter selectron. Compared to the MSSM there are not so many solutions in the NMSSM with small chargino mass and large selectron mass following from the suppression of the domain $m_0 \gg |m_{1/2}|$ in the NMSSM as discussed in [9]. In the lower right picture the dark matter

condition is imposed leading to an upper bound of 500 GeV for the lighter chargino and a cosmologically allowed mass range of $100 \text{ GeV} < m_{\tilde{e}_R} < 450 \text{ GeV}$ for the lighter selectron in the NMSSM. The cosmologically allowed solutions in the MSSM and NMSSM show some differences. Only in the MSSM there are cosmologically allowed heavier selectrons. In contrast to the MSSM, the dark matter condition leads to a slightly improved lower bound of 90 GeV for the lighter chargino in the NMSSM. The reason is the enhanced lower bound of 50 GeV for the cosmologically allowed LSP neutralinos in the NMSSM as discussed and shown in Fig.4 and the proportionality between the mass of the lighter chargino and the mass of the bino-like LSP neutralino.

In the upper left picture of Fig.6 the mass of the lighter u-squark versus the gluino mass is shown for the MSSM. The upper boundary line for the lighter u-squark mass results from the restriction of m_0 . As mentioned in section 3 we have chosen m_0 to be smaller than 1500 GeV in order to avoid too much finetuning. The lower bound for the gluino and the lighter u-squark is 250 GeV . In the upper right picture the cosmologically allowed lighter u-squark masses are shown. In many cases the cosmologically allowed lighter u-squark mass is proportional to the gluino mass. The deviations from proportionality with large u-squark masses follow from the Z-poles or Higgs-poles shown in the upper right picture of Fig.1. The dark matter condition leads to an upper bound of 1600 GeV for the gluino following from the cosmological upper bound of 240 GeV for the bino-like LSP neutralino. In the lower left picture the mass of the lighter u-squark is shown for the NMSSM. In contrast to the MSSM [43], the squark masses in the NMSSM are nearly proportional to the gluino mass as discussed in [20]. The reason is, that in the NMSSM solutions with $m_0 \gg |m_{1/2}|$ are somewhat disfavored. In contrast to the MSSM the lower bound for the gluino is 330 GeV in the NMSSM, which follows from the lower experimental bound of 85.4 GeV [28] for the chargino and from the lower bound of about 2.4 for $|\tan \beta|$ in the NMSSM (see Fig.8) as discussed in [9]. Excluding small values of m_0 the UFB-3 constraint (Eq.(27)) further improves the lower bound for the lighter u-squark to 370 GeV . In the lower right picture the dark matter condition is imposed. In contrast to the MSSM, the dark matter condition improves the lower bound for the gluino to 370 GeV in the NMSSM as discussed in [20]. The reason is the enhanced lower bound of 50 GeV and the larger

Higgsino portion of the lightest cosmologically allowed LSP neutralinos in the NMSSM. With the dark matter condition the lower bound for the lighter u-squark slightly improves to 390 GeV . The cosmological upper bound of 1800 GeV for the gluino in the NMSSM is similar to the corresponding upper bound in the MSSM. The upper bound of 1600 GeV for the lighter u-squark in the NMSSM corresponds to the upper bound for the lighter u-squark in the MSSM at large gluino masses.

In the upper left picture of Fig.7 the mass of the lighter stop versus the gluino mass is shown for the MSSM. The stop masses are restricted from above, since the m_0 values have been chosen to be smaller than 1500 GeV as discussed in section 3. In the upper right picture the cosmologically allowed lighter stop masses are shown. Large stop masses at moderate gluino masses are allowed due to Z-poles and Higgs-poles. The dark matter condition sets an upper bound of 1200 GeV for the lighter stop at large gluino masses. In the lower left picture the lighter stop masses are shown for the NMSSM. In contrast to the MSSM [43], the lighter stop mass is nearly proportional to the gluino mass as discussed in [20] following from the suppression of the domain $m_0 \gg |m_{1/2}|$ in the NMSSM. In addition the constraints for the trilinear couplings A_{u_i} , A_{d_i} and A_{e_i} (Eqs.(17)-(19)) are stronger in the NMSSM than in the MSSM. The corresponding constraints in the MSSM are obtained by replacing $m_{H_{1,2}}^2$ in (Eqs.(17)-(19)) by $m_{H_{1,2}}^2 + \mu^2$. The stronger constraints for the trilinear couplings lead to a larger mass of the stop in the NMSSM, since the stop mixing depends on A_t . Together with the UFB-3 constraint (Eq.(27)), which excludes small values of m_0 , the lower bound for the lighter stop increases to 240 GeV in the NMSSM. The lower right picture shows the cosmologically restricted solutions. The lower bound for the lighter stop slightly improves to 270 GeV . The cosmological upper bound of 1300 GeV for the lighter stop in the NMSSM is similar to the corresponding upper bound for the lighter stop in the MSSM at large gluino masses.

In the upper left picture of Fig.8 we show the mass of the lighter scalar Higgs S_1 versus $|\tan\beta|$ for the MSSM. In the MSSM the mass of the scalar Higgs S_1 has to be larger than the lower experimental bound of 64.5 GeV [30]. The upper bound for m_{S_1} is 155 GeV . For $|\tan\beta|$ there is a lower bound of about 1.4. In the upper right picture the dark

matter condition is imposed improving the upper bound for m_{S_1} to about 145 GeV . The lower left picture shows the mass of the lightest scalar Higgs S_1 in the NMSSM, which is lower than 150 GeV . Before applying the UFB-3 constraint (Eq.(27)) there exist scalar Higgses S_1 in the NMSSM lighter than the MSSM Higgs bound of 64.5 GeV [30], which are predominantly a Higgs singlet N [8, 11, 12]. These very light scalar Higgses are now excluded by the UFB-3 constraint (Eq.(27)), which excludes the parameter region with small m_0 and large $|m_{1/2}|$. But this parameter region is needed in order to have very light scalar Higgses with a large Higgs singlet portion [13]. In contrast to the MSSM, the lower bound for $|\tan \beta|$ in the NMSSM is about 2.4. The higher lower bound for $|\tan \beta|$ follows from the extra third minimum condition (Eq.(11)) in the NMSSM. For larger values of $|\tan \beta|$ the density of NMSSM solutions decreases, if the UFB-3 constraint (Eq.(27)) is applied. This follows from the fact that the NMSSM solutions with larger $|\tan \beta|$ are lying in the parameter region with small m_0 and large $|m_{1/2}|$ [9, 10]. The lower right picture shows only solutions, which fulfill the dark matter condition. In the NMSSM the cosmologically allowed scalar Higgs S_1 is heavier than 69 GeV and lighter than 130 GeV . In contrast to the MSSM the dark matter condition together with the UFB-3 constraint (Eq.(27)) leads to an upper bound of about 9 for $|\tan \beta|$ in the NMSSM. However our investigations are restricted to $|\tan \beta|$ values below 20 as mentioned in section 3.

In the upper left picture of Fig.9 we show the mass of the lighter scalar Higgs S_1 versus the mass of the pseudoscalar Higgs P_1 for the MSSM. In the MSSM m_{P_1} is larger than 150 GeV within our restricted range of $|\tan \beta|$ values below 20 as mentioned in section 3. The upper right picture shows the cosmologically allowed Higgses. The dark matter condition restricts the mass of the pseudoscalar Higgs P_1 to the range $200 \text{ GeV} < m_{P_1} \lesssim 2300 \text{ GeV}$. The lower left picture shows the mass of the lightest scalar Higgs S_1 versus the mass of the lighter pseudoscalar Higgs P_1 for the NMSSM. If the UFB-3 constraint (Eq.(27)) is not applied there exist very light scalar Higgses S_1 correlated with very light pseudoscalar Higgses P_1 which have both a large Higgs singlet portion [8]. With the UFB-3 constraint (Eq.(27)) these very light Higgses are now excluded as already discussed for the very light scalar Higgs S_1 (see Fig.8). For this reason we have now a lower bound of 200 GeV for the pseudoscalar Higgs P_1 in the NMSSM for $|\tan \beta|$ values below 20. In the lower right

picture the dark matter condition is imposed leading to a lower bound of 250 GeV and an upper bound of 900 GeV for the lighter pseudoscalar Higgs P_1 . Compared with the MSSM the upper bound for the lighter pseudoscalar Higgs P_1 is somewhat lower in the NMSSM. This follows from the extra third minimum condition (Eq.(11)) in the NMSSM and the suppression of the domain $m_0 \gg |m_{1/2}|$ in the NMSSM.

7 Conclusions

In the present paper we have made a comparison between the MSSM and NMSSM concerning the parameter space and the particle spectra. In contrast to the MSSM, the case $m_0 \gg |m_{1/2}|$ is disfavored in the NMSSM as discussed in [9] and the squark masses are nearly proportional to the gluino mass (cf. Figs.(6) and (7)). Furthermore the gluino and the lighter u-squark in the NMSSM are heavier than in the MSSM. In the NMSSM the lower bound for the gluino is 330 GeV and 370 GeV for the lighter u-squark, whereas the lower bound for the gluino and lighter u-squark in the MSSM is 250 GeV . In the NMSSM a light stop is excluded by the stronger constraints for the trilinear couplings A_{u_i} , A_{d_i} and A_{e_i} (Eqs.(17)-(19)) and the UFB-3 constraint (Eq.(27)). This leads to a larger stop mass $m_{\tilde{t}_1} > 240 \text{ GeV}$ in the NMSSM even before considering dark matter constraints. This is in contrast to the MSSM where stops as light as the experimental lower bound of 63 GeV [25] are allowed. One important difference between the NMSSM and the MSSM is the occurrence of LSP singlinos and light scalar and pseudoscalar Higgs singlets in the NMSSM. Applying the UFB-3 constraint (Eq.(27)) these singlet states are excluded as shown in Fig.4 and Fig.9 and discussed in section 6. In this way the UFB-3 constraint strongly reduces the differences between the NMSSM and the MSSM.

Furthermore we have investigated the consequences of the dark matter condition for the MSSM and NMSSM. Together with the UFB-3 constraint (Eq.(27)) the dark matter condition gives an upper bound of about 9 for $|\tan\beta|$ in the NMSSM (see Fig.8), whereas in the MSSM larger values of $|\tan\beta|$ are furthermore allowed within our investigated range of $|\tan\beta|$ values below 20. For the LSP neutralinos, lightest charginos, gluinos and scalar Higgses S_1 the cosmologically allowed mass ranges are comparable for the MSSM

($40 \text{ GeV} < m_{\tilde{\chi}_1^0} < 240 \text{ GeV}$, $85.4 \text{ GeV} < m_{\tilde{\chi}_1^\pm} < 450 \text{ GeV}$, $250 \text{ GeV} < m_{\tilde{g}} < 1600 \text{ GeV}$, $64.5 \text{ GeV} < m_{S_1} < 145 \text{ GeV}$) and for the NMSSM ($50 \text{ GeV} < m_{\tilde{\chi}_1^0} < 260 \text{ GeV}$, $90 \text{ GeV} < m_{\tilde{\chi}_1^\pm} < 500 \text{ GeV}$, $370 \text{ GeV} < m_{\tilde{g}} < 1800 \text{ GeV}$, $69 \text{ GeV} < m_{S_1} < 130 \text{ GeV}$). The enhanced lower bound of 50 GeV and the larger Higgsino portion of the lightest cosmologically allowed LSP neutralinos leads to improved lower bounds for the charginos and gluinos in the NMSSM. Furthermore the dark matter condition slightly improves the lower bounds for the lighter u-squark and lighter stop in the NMSSM to 390 GeV and 270 GeV , respectively. In the MSSM, due to Z-pole and Higgs-pole enhanced neutralino pair annihilation, large masses of the selectrons, u-squarks and stops are cosmologically allowed. In contrast, the NMSSM does not allow for large slepton and squark masses at moderate gluino masses (cf. Figs.(5-7)) and the dark matter condition leads to the upper bounds $m_{\tilde{e}_R} < 450 \text{ GeV}$, $m_{\tilde{u}_R} < 1600 \text{ GeV}$ and $m_{\tilde{t}_1} < 1300 \text{ GeV}$ at large gluino masses, which are comparable with the MSSM. In comparison with the MSSM the upper bound for the cosmologically allowed pseudoscalar Higgs P_1 is somewhat lower in the NMSSM $m_{P_1} < 900 \text{ GeV}$ (Fig.9).

Despite of the discussed differences, it may be difficult to distinguish experimentally between the MSSM and NMSSM. One possibility is the measurement of smaller couplings of the neutral Higgses in the NMSSM, which result from the mixing of the ordinary Higgs states with the Higgs singlets as discussed in [8, 9] and [11] - [13]. Another possibility suggested in [9, 10] is the search for an additional cascade in the NMSSM, which is produced in the decay of the bino-like second lightest neutralino into the LSP singlino. Since the LSP singlinos are excluded by the UFB-3 constraint this additional cascade is not a way to discriminate between the NMSSM and MSSM any more.

Acknowledgements

I am grateful to M. Glück and E. Reya for suggestions and many helpful discussions. Also I would like to thank U. Ellwanger and C.A. Savoy for useful conversations. The work has been supported by the 'Graduiertenkolleg am Institut für Physik der Universität Dortmund'.

Appendix A1: Annihilation cross section

To calculate the relic neutralino density (Eq.(30)) in the NMSSM we need the annihilation cross section of the neutralinos into the different decay products X and Y .

$$\tilde{\chi}_1^0(h) \tilde{\chi}_1^0(\bar{h}) \rightarrow X(\lambda_X) Y(\lambda_Y)$$

$\lambda_f = \lambda_X - \lambda_Y$, where λ_X and λ_Y are the helicities of particle X and Y . Within the partial wave formalism the annihilation cross section is obtained [34] as:

$$\sigma_{ann}(\tilde{\chi}_1^0 \tilde{\chi}_1^0 \rightarrow X Y)v = \frac{1}{4} \frac{\bar{\beta}_f}{8\pi s S} \left[|A(^1S_0)|^2 + \frac{1}{3} (|A(^3P_0)|^2 + |A(^3P_1)|^2 + |A(^3P_2)|^2) \right] \quad (34)$$

$$\bar{\beta}_f = \sqrt{1 - \frac{2(m_X^2 + m_Y^2)}{s} + \frac{(m_X^2 - m_Y^2)^2}{s^2}} \quad (35)$$

$s \approx 4m_{\tilde{\chi}}^2$ is the center of mass energy squared. S is a symmetry factor, which is 2 if $X = Y$. Summation over final helicities is implicit in Eq.(34). The partial wave amplitude $A(^{2S+1}L_J)$ describes annihilation from an initial state with spin S , orbital angular momentum L and total angular momentum J . The partial wave amplitudes $A(^{2S+1}L_J)$ for the NMSSM are obtained by slightly modifying the partial wave amplitudes of the MSSM in [34] and by using the corresponding NMSSM couplings. Thereby we have corrected some misprints [44] in [34]. One modification of the neutralino annihilation is the exchange of 5 neutralinos in the NMSSM instead of 4 neutralinos in the MSSM. Other modifications concern the exchange of the scalar Higgses S_1 , S_2 and S_3 in the NMSSM instead of H_1 and H_2 in the MSSM and the exchange of the pseudoscalar Higgses P_1 and P_2 in the NMSSM instead of P in the MSSM. In addition the NMSSM coupling $g_{\alpha-+}$ (Eq.(98)) has to be inserted in Eq.(86). In the MSSM there is only one pseudoscalar Higgs P and the coupling $g_{\alpha-+}$ turns out to be 1. In the following the partial wave amplitudes $A(^{2S+1}L_J)$ of the NMSSM for all decay channels are given in leading order in the relative velocity v of the non-relativistic neutralinos. Previously we give some NMSSM couplings and definitions. The couplings of the W boson to the chargino $\tilde{\chi}_j^+$ and the LSP neutralino, which is denoted with index 0 in [34] instead of 1, have the same form in the MSSM and NMSSM, but a different matrix N (Eq.(15)) enters:

$$O_{0j}^L = -\frac{1}{\sqrt{2}} N_{04} V_{j2} + N_{02} V_{j1} \quad (36)$$

$$O_{0j}^R = \frac{1}{\sqrt{2}} N_{03} U_{j2} + N_{02} U_{j1}. \quad (37)$$

The mass matrix of the charginos is diagonalized by the orthogonal matrices U and V , which are explicitly given in [40]. In the NMSSM the couplings of the charged Higgs to the chargino $\tilde{\chi}_j^+$ and the LSP neutralino has to be modified compared to the MSSM:

$$Q_{0j}^L = N_{04} V_{j1} + \frac{1}{\sqrt{2}} (N_{02} + N_{01} \tan \theta_W) V_{j2} - \frac{\lambda \tan \beta}{g_2} N_{05} V_{j2} \quad (38)$$

$$Q_{0j}^R = N_{03} U_{j1} - \frac{1}{\sqrt{2}} (N_{02} + N_{01} \tan \theta_W) U_{j2} - \frac{\lambda}{g_2 \tan \beta} N_{05} U_{j2}. \quad (39)$$

In the MSSM and NMSSM the coupling of the Z boson to the neutralinos $\tilde{\chi}_i^0$ and $\tilde{\chi}_j^0$ is given by:

$$O_{ij}^{\prime L} = -\frac{1}{2} N_{i3} N_{j3} + \frac{1}{2} N_{i4} N_{j4}. \quad (40)$$

In the NMSSM the coupling of the scalar Higgs S_a to the neutralinos $\tilde{\chi}_i^0$ and $\tilde{\chi}_j^0$ changes compared to the MSSM and can be written as:

$$T_{S_a ij} = -U_{a1}^S Q_{ij}'' + U_{a2}^S S_{ij}'' + U_{a3}^S Z_{ij}'' \quad (41)$$

$$Q_{ij}'' = \frac{1}{2 g_2} [N_{i3} (g_2 N_{j2} - g_y N_{j1}) + \sqrt{2} \lambda N_{i4} N_{j5} + (i \leftrightarrow j)] \quad (42)$$

$$S_{ij}'' = \frac{1}{2 g_2} [N_{i4} (g_2 N_{j2} - g_y N_{j1}) - \sqrt{2} \lambda N_{i3} N_{j5} + (i \leftrightarrow j)] \quad (43)$$

$$Z_{ij}'' = \frac{1}{2 g_2} [-\sqrt{2} \lambda N_{i3} N_{j4} + \sqrt{2} k N_{i5} N_{j5} + (i \leftrightarrow j)]. \quad (44)$$

The 3×3 mass matrix of the scalar Higgses S_i [3] in the basis $(H_{1R}^0, H_{2R}^0, N_R)$ with $H_{iR}^0 = \sqrt{2} \text{Re}\{H_i^0\}$ ($i = 1 - 3$) is diagonalised by the matrix U^S . The scalar Higgses S_i ($i = 1 - 3$) are ordered with increasing mass. The coupling of the pseudoscalar Higgs P_α to the neutralinos is also different in the MSSM and NMSSM. In the NMSSM this coupling has the following form:

$$T_{P_\alpha ij} = -U_{\alpha 1}^P Q_{ij}''' + U_{\alpha 2}^P S_{ij}''' - U_{\alpha 3}^P Z_{ij}''' \quad (45)$$

$$Q_{ij}''' = \frac{1}{2g_2} [N_{i3} (g_2 N_{j2} - g_y N_{j1}) - \sqrt{2} \lambda N_{i4} N_{j5} + (i \leftrightarrow j)] \quad (46)$$

$$S_{ij}''' = \frac{1}{2g_2} [N_{i4} (g_2 N_{j2} - g_y N_{j1}) + \sqrt{2} \lambda N_{i3} N_{j5} + (i \leftrightarrow j)] \quad (47)$$

$$Z_{ij}''' = Z_{ij}'' \quad (48)$$

The 3×3 mass matrix of the pseudoscalar Higgses P_α and the neutral Goldstone boson [3] in the basis $(H_{1I}^0, H_{2I}^0, N_I)$ with $H_{iI}^0 = \sqrt{2} \text{Im}\{H_i^0\}$ ($i = 1-3$) is here diagonalised by the 3×3 matrix U^P . The pseudoscalar Higgses P_α ($i = 1, 2$) are ordered with increasing mass. In [34] the following definitions are used:

$$\Delta^2 = \frac{m_X^2 + m_Y^2}{2m_{\tilde{\chi}}^2} \quad (49)$$

$$R_X = \frac{m_X}{m_{\tilde{\chi}}}, \text{ etc.} \quad (50)$$

$$P_I = 1 + R_I^2 - (R_X^2 + R_Y^2)/2. \quad (51)$$

1. $\tilde{\chi}_1^0 \tilde{\chi}_1^0 \rightarrow W^-(\lambda) W^+(\bar{\lambda})$.

The W bosons are produced by Z boson and scalar Higgs S_i ($i = 1, 2, 3$) exchange in the s-channel and chargino $\tilde{\chi}_j^\pm$ ($j = 1, 2$) exchange in the t- and u-channel.

$A(^1S_0) : \lambda_f = 0, \lambda = \pm 1$

$$2\sqrt{2}\bar{\beta}_f g_2^2 \frac{O_{0j}^{L2} + O_{0j}^{R2}}{P_j} + \sqrt{2}v^2\bar{\beta}_f g_2^2 \left[\frac{2}{3} \frac{R_j^+}{P_j^2} O_{0j}^L O_{0j}^R + \frac{O_{0j}^{L2} + O_{0j}^{R2}}{P_j} \left[\frac{1}{4} - \frac{4}{3P_j} + \frac{2\bar{\beta}_f^2}{3P_j^2} \right] \right] \quad (52)$$

$A(^3P_0) : \lambda_f = 0, \lambda = 0$

$$\frac{\sqrt{6}v g_2^2}{R_W^2} \left[-\frac{4}{3} \frac{O_{0j}^{L2} + O_{0j}^{R2}}{P_j} + \frac{4O_{0j}^L O_{0j}^R R_j^+}{P_j} \left[1 - \frac{2}{3P_j} \right] \right]$$

$$\begin{aligned}
& + \sqrt{6} v g_2^2 \left[\frac{O_{0j}^{L2} + O_{0j}^{R2}}{P_j} \left[1 - \frac{2\bar{\beta}_f^2}{3P_j} \right] - \frac{2O_{0j}^L O_{0j}^R R_j^+}{P_j} \left[1 - \frac{4}{3P_j} \right] \right] \\
& - \frac{\sqrt{6} v (1 + \bar{\beta}_f^2) g_2^2 F_i}{(4 - R_{S_i}^2 + iG_{S_i}) R_W}
\end{aligned} \tag{53}$$

$$\lambda_f = 0, \lambda = \pm 1$$

$$\sqrt{6} v g_2^2 \left[\frac{O_{0j}^{L2} + O_{0j}^{R2}}{P_j} \left[\frac{1}{3} - \frac{2\bar{\beta}_f^2}{3P_j} \right] - \frac{2O_{0j}^L O_{0j}^R R_j^+}{P_j} \right] + \frac{\sqrt{6} v g_2^2 R_W F_i}{4 - R_{S_i}^2 + iG_{S_i}} \tag{54}$$

$$A(^3P_1) : |\lambda_f| = 1$$

$$\begin{aligned}
& \frac{2v\bar{\beta}_f^2 \lambda_f g_2^2}{R_W} \left[\frac{O_{0j}^{L2} + O_{0j}^{R2}}{P_j} \left[1 - \frac{1}{P_j} \right] - \frac{2O_{0j}^L O_{0j}^R R_j^+}{P_j^2} \right] \\
& + 2v\bar{\beta}_f g_2^2 \frac{O_{0j}^{L2} - O_{0j}^{R2}}{R_W P_j} \left[2 - \frac{\bar{\beta}_f^2}{P_j} \right] - \frac{8v\bar{\beta}_f g_2^2 O_{00}''L}{R_W (4 - R_Z^2)}
\end{aligned} \tag{55}$$

$$\lambda_f = 0, \lambda = 0$$

$$\frac{2v\bar{\beta}_f}{R_W^2 P_j} (3 - \bar{\beta}_f^2) g_2^2 (O_{0j}^{L2} - O_{0j}^{R2}) - \frac{4v\bar{\beta}_f g_2^2 O_{00}''L}{(4 - R_Z^2) R_W^2} (3 - \bar{\beta}_f^2) \tag{56}$$

$$\lambda_f = 0, \lambda = \pm 1$$

$$\frac{2v\bar{\beta}_f}{P_j} g_2^2 (O_{0j}^{L2} - O_{0j}^{R2}) - \frac{4v\bar{\beta}_f g_2^2 O_{00}''L}{4 - R_Z^2} \tag{57}$$

$$A(^3P_2) : |\lambda_f| = 2$$

$$- \frac{2\sqrt{2}v}{P_j} g_2^2 (O_{0j}^{L2} + O_{0j}^{R2}) \tag{58}$$

$$|\lambda_f| = 1$$

$$\frac{2v g_2^2}{R_W} \left[\frac{-R_j^{+2}}{P_j^2} (O_{0j}^{L2} + O_{0j}^{R2}) + \frac{2O_{0j}^L O_{0j}^R R_j^+}{P_j^2} \bar{\beta}_f^2 + \lambda_f \bar{\beta}_f^3 \frac{O_{0j}^{L2} - O_{0j}^{R2}}{P_j^2} \right] \tag{59}$$

$$\lambda_f = 0, \lambda = \pm 1$$

$$\frac{2v g_2^2}{\sqrt{3}} (O_{0j}^{L2} + O_{0j}^{R2}) \frac{1 - R_j^{+2} - R_W^2}{P_j^2} \quad (60)$$

$$\lambda_f = 0, \lambda = 0$$

$$\frac{4v g_2^2}{\sqrt{3} R_W^2} \left[-\frac{O_{0j}^{L2} + O_{0j}^{R2}}{P_j} \left[1 - \bar{\beta}_f^2 \frac{R_W^2}{P_j} \right] + 4 \bar{\beta}_f^2 \frac{O_{0j}^L O_{0j}^R R_j^+}{P_j^2} \right] \quad (61)$$

$G_{S_i} = \Gamma_{S_i} m_{S_i} / m_{\tilde{\chi}}^2$ are the rescaled widths of the scalar Higgses S_i . The coupling of the scalar Higgs S_i to the LSP neutralinos and to the W bosons is combined to F_i . In the NMSSM F_i is given by:

$$F_i = (U_{i1}^S \cos \beta + U_{i2}^S \sin \beta) T_{S_i 00}. \quad (62)$$

$$2. \quad \tilde{\chi}_1^0 \tilde{\chi}_1^0 \rightarrow Z(\lambda) Z(\bar{\lambda}).$$

The Z bosons are produced by scalar Higgs S_i ($i = 1, 2, 3$) exchange in the s-channel and neutralino $\tilde{\chi}_j^0$ ($j = 1 - 5$) exchange in the t- and u-channel.

$$A(^1S_0) : \lambda_f = 0, \lambda = \pm 1$$

$$\frac{4\sqrt{2} \bar{\beta}_f g_2^2 O_{0j}^{\prime L2}}{\cos^2 \theta_W P_j} + \frac{2\sqrt{2} v^2 \bar{\beta}_f g_2^2 O_{0j}^{\prime L2}}{\cos^2 \theta_W} \left[-\frac{R_j}{3 P_j^2} + \frac{1}{P_j} \left[\frac{1}{4} - \frac{4}{3 P_j} + \frac{2 \bar{\beta}_f^2}{3 P_j^2} \right] \right] \quad (63)$$

$$A(^3P_0) : \lambda_f = 0, \lambda = 0$$

$$\begin{aligned} & \frac{4\sqrt{6} v g_2^2}{\cos^2 \theta_W R_Z^2} O_{0j}^{\prime L2} \left[-\frac{2}{3 P_j} - \frac{R_j}{P_j} \left[1 - \frac{2}{3 P_j} \right] \right] \\ & + \frac{2\sqrt{6} v g_2^2 O_{0j}^{\prime L2}}{\cos^2 \theta_W} \left[\frac{1}{P_j} \left[1 - \frac{2 \bar{\beta}_f^2}{3 P_j} \right] + \frac{R_j}{P_j} \left[1 - \frac{4}{3 P_j} \right] \right] - \frac{\sqrt{6} v g_2^2 (1 + \bar{\beta}_f^2) F_i}{(4 - R_{S_i}^2 + i G_{S_i}) R_W} \end{aligned} \quad (64)$$

$$\lambda_f = 0, \lambda = \pm 1$$

$$\frac{2\sqrt{6} v g_2^2 O_{0j}^{\prime L2}}{\cos^2 \theta_W} \left[\frac{1}{P_j} \left[\frac{1}{3} - \frac{2 \bar{\beta}_f^2}{3 P_j} \right] + \frac{R_j}{P_j} \right] + \frac{\sqrt{6} v g_2^2 R_W F_i}{\cos^2 \theta_W (4 - R_{S_i}^2 + i G_{S_i})} \quad (65)$$

$$A(^3P_1) : |\lambda_f| = 1$$

$$\frac{4 v \bar{\beta}_f^2 \lambda_f g_2^2 O_{0j}^{\prime\prime L2}}{\cos^2 \theta_W R_Z} \left[\frac{1}{P_j} \left[1 - \frac{1}{P_j} \right] + \frac{R_j}{P_j^2} \right] \quad (66)$$

$$A(^3P_2) : |\lambda_f| = 2$$

$$- \frac{4 \sqrt{2} v g_2^2}{\cos^2 \theta_W P_j} O_{0j}^{\prime\prime L2} \quad (67)$$

$$|\lambda_f| = 1$$

$$- \frac{4 v g_2^2}{\cos^2 \theta_W R_Z} O_{0j}^{\prime\prime L2} \left[\frac{R_j^2}{P_j^2} + \frac{R_j}{P_j^2} \bar{\beta}_f^2 \right] \quad (68)$$

$$\lambda_f = 0, \lambda = \pm 1$$

$$\frac{4 v g_2^2}{\sqrt{3} \cos^2 \theta_W} O_{0j}^{\prime\prime L2} \frac{1 - R_j^2 - R_Z^2}{P_j^2} \quad (69)$$

$$\lambda_f = 0, \lambda = 0$$

$$- \frac{8 v g_2^2}{\sqrt{3} \cos^2 \theta_W R_Z^2} O_{0j}^{\prime\prime L2} \left[\frac{1}{P_j} \left[1 - \frac{R_Z^2 \bar{\beta}_f^2}{P_j} \right] + \frac{2 R_j \bar{\beta}_f^2}{P_j^2} \right] \quad (70)$$

$$3. \quad \tilde{\chi}_1^0 \tilde{\chi}_1^0 \rightarrow Z(\lambda) S_a.$$

The Z boson and the scalar Higgs S_a are produced by Z boson and pseudoscalar Higgs P_α ($\alpha = 1, 2$) exchange in the s-channel and neutralino $\tilde{\chi}_j^0$ ($j = 1 - 5$) exchange in the t- and u-channel.

$$A(^1S_0) : \lambda = 0$$

$$\begin{aligned} & - \frac{2 \sqrt{2} \bar{\beta}_f}{R_Z} \frac{g_2^2}{\cos \theta_W} \left[\frac{2 J_j (R_j - 1)}{P_j} + \frac{O}{R_Z \cos \theta_W} - \frac{4 L_\alpha}{4 - R_{P_\alpha}^2 + i G_{P_\alpha}} \right] \\ & - v^2 \frac{\sqrt{2} \bar{\beta}_f}{R_Z} \frac{g_2^2}{\cos \theta_W} \frac{J_j}{P_j} \left[\frac{1}{2} (R_j - 5) - \frac{2 (R_j - 1)}{P_j} + \frac{4 (R_j - 1)}{3 P_j^2} \bar{\beta}_f^2 + (2 - \Delta^2) \frac{2}{3 P_j} \right] \end{aligned}$$

$$+ v^2 \frac{\sqrt{2} \bar{\beta}_f}{R_Z} \frac{g_2^2}{\cos \theta_W} \left[\frac{3 L_\alpha}{4 - R_{P_\alpha}^2 + i G_{P_\alpha}} - \frac{O}{4 R_Z \cos \theta_W} \right] \quad (71)$$

$A(^3P_1) : \lambda = \pm 1$

$$- 4 v \frac{g_2^2}{\cos \theta_W} \frac{J_j}{P_j^2} \left[R_j^2 - \frac{\delta^4}{4} \right] - 4 v \frac{g_2^2}{\cos \theta_W} \frac{J_j R_j}{P_j} + 2 v \frac{g_2^2}{\cos^2 \theta_W} O \frac{R_Z}{4 - R_Z^2} \quad (72)$$

$\lambda = 0$

$$- 2 \frac{v}{R_Z} \left[1 + \frac{\delta^2}{2} \right] \frac{g_2^2}{\cos \theta_W} \left[2(1 + R_j) \frac{J_j}{P_j} - \frac{R_Z}{\cos \theta_W (4 - R_Z^2)} O \right] \quad (73)$$

$A(^3P_2) : \lambda = \pm 1$

$$- 4 \lambda v \bar{\beta}_f^2 \frac{g_2^2}{\cos \theta_W} \frac{J_j}{P_j^2} \quad (74)$$

In [34] the following definition is used:

$$\delta^2 = (R_Z^2 - R_{S_a}^2)/2. \quad (75)$$

$G_{P_\alpha} = \Gamma_{P_\alpha} m_{P_\alpha} / m_{\tilde{\chi}}^2$ are the rescaled widths of the pseudoscalar Higgses P_α . The couplings appearing in the neutralino $\tilde{\chi}_j^0$ exchange are combined to J_j :

$$J_j = -O_{0j}^{\prime L} T_{S_a 0j}. \quad (76)$$

L_α is the product of the coupling of the pseudoscalar Higgs P_α to the LSP neutralinos and to the Z boson and the scalar Higgs S_a . In the NMSSM L_α reads:

$$L_\alpha = \frac{1}{2} (U_{a2}^S U_{\alpha 2}^P - U_{a1}^S U_{\alpha 1}^P) T_{P_\alpha 00}. \quad (77)$$

O consists of the couplings appearing in the Z boson exchange. In the NMSSM O is given by:

$$O = O_{00}^{\prime L} (U_{a1}^S \cos \beta + U_{a2}^S \sin \beta). \quad (78)$$

$$4. \quad \tilde{\chi}_1^0 \tilde{\chi}_1^0 \rightarrow Z(\lambda) P_\alpha.$$

The Z boson and the pseudoscalar Higgs P_α are produced by scalar Higgs S_i ($i = 1, 2, 3$) exchange in the s-channel and neutralino $\tilde{\chi}_j^0$ ($j = 1 - 5$) exchange in the t- and u-channel.

$$A(^3P_0) : \lambda = 0$$

$$4\sqrt{6} \frac{v \bar{\beta}_f}{R_Z} \frac{g_2^2}{\cos \theta_W} \left[\left[1 + \frac{\delta^2}{2} \right] \frac{K_j R_j}{3 P_j^2} - \left[\frac{2}{3} + R_j^2 - \frac{2 \Delta^2}{3} + \frac{\delta^2}{6} \right] \frac{K_j}{P_j^2} + \frac{L_i}{4 - R_{S_i}^2} \right] \quad (79)$$

$$A(^3P_1) : \lambda = \pm 1$$

$$- 4 v \bar{\beta}_f \lambda \frac{g_2^2}{\cos \theta_W} \left[-R_j + \frac{\delta^2}{2} \right] \frac{K_j}{P_j^2} \quad (80)$$

$$A(^3P_2) : \lambda = \pm 1$$

$$4 v \bar{\beta}_f \frac{g_2^2}{\cos \theta_W} \left[-R_j + \frac{\delta^2}{2} \right] \frac{K_j}{P_j^2} \quad (81)$$

$$\lambda = 0$$

$$- \frac{8}{\sqrt{3}} v \bar{\beta}_f \frac{g_2^2}{\cos \theta_W} \frac{K_j}{R_Z P_j^2} \left[1 + R_j - \Delta^2 + \frac{\delta^2}{2} (R_j - 1) \right] \quad (82)$$

In [34] the following definition is used:

$$\delta^2 = (R_Z^2 - R_{P_\alpha}^2)/2. \quad (83)$$

The couplings appearing in the neutralino $\tilde{\chi}_j^0$ exchange are combined to K_j :

$$K_j = O_{0j}^{\prime\prime L} T_{P_\alpha 0j}. \quad (84)$$

L_i is the product of the coupling of the scalar Higgs S_i to the LSP neutralinos and to the Z boson and the pseudoscalar Higgs P_α . In the NMSSM L_i has the following form:

$$L_i = \frac{1}{2} (U_{i2}^S U_{\alpha 2}^P - U_{i1}^S U_{\alpha 1}^P) T_{S_i 00}. \quad (85)$$

$$5. \quad \tilde{\chi}_1^0 \tilde{\chi}_1^0 \rightarrow W^-(\lambda) H^+.$$

The W boson and charged Higgs are produced by scalar Higgs S_i ($i = 1, 2, 3$) and pseudoscalar Higgs P_α ($\alpha = 1, 2$) exchange in the s-channel and chargino $\tilde{\chi}_j^+$ ($j = 1, 2$) exchange in the t- and u-channel.

$$A(^1S_0) : \lambda = 0$$

$$\begin{aligned} & 4\sqrt{2}\bar{\beta}_f g_2^2 \frac{J'_j + J''_j}{R_W P_j} + \sqrt{2}v^2 \frac{\bar{\beta}_f g_2^2 (J'_j + J''_j)}{R_W P_j} \left[\frac{5}{2} - \frac{2}{P_j} + \frac{4\bar{\beta}_f^2}{3P_j^2} - \frac{2}{3P_j} (2 - \Delta^2) \right] \\ & - 4\sqrt{2}\bar{\beta}_f g_2^2 (J'_j - J''_j) \frac{R_j^+}{R_W P_j} - \sqrt{2}\bar{\beta}_f v^2 g_2^2 (J'_j - J''_j) \frac{R_j^+}{R_W P_j} \left[\frac{4\bar{\beta}_f^2}{3P_j^2} - \frac{2}{P_j} + \frac{1}{2} \right] \\ & - 4\sqrt{2}\bar{\beta}_f g_2^2 g_{\alpha--} T_{P_\alpha 00} \frac{1}{R_W} \frac{1}{4 - R_{P_\alpha}^2} \left[1 + \frac{3v^2}{8} \right] \end{aligned} \quad (86)$$

$$A(^3P_0) : \lambda = 0$$

$$\begin{aligned} & 4\sqrt{6} \frac{v\bar{\beta}_f}{R_W} g_2^2 \left[R_j^+ \left[1 + \frac{\delta^2}{2} \right] \frac{K'_j - K''_j}{3P_j^2} - \left[\frac{2}{3} + R_j^{+2} - \frac{2}{3}\Delta^2 + \frac{\delta^2}{6} \right] \frac{K'_j + K''_j}{P_j^2} \right] \\ & - \frac{4\sqrt{6}}{R_W} v\bar{\beta}_f \frac{g_2^2 L_i}{4 - R_{S_i}^2} \end{aligned} \quad (87)$$

$$A(^3P_1) : \lambda = \pm 1$$

$$\begin{aligned} & -4v \left[R_j^{+2} - \frac{\delta^4}{4} \right] g_2^2 \frac{J'_j + J''_j}{P_j^2} - 4v g_2^2 (J'_j - J''_j) \frac{R_j^+}{P_j} \\ & + \frac{4v\bar{\beta}_f \lambda}{P_j^2} g_2^2 \left[R_j^+ (K'_j - K''_j) - \frac{\delta^2}{2} (K'_j + K''_j) \right] \end{aligned} \quad (88)$$

$$\lambda = 0$$

$$- \frac{4v g_2^2}{R_W P_j} \left[(J'_j + J''_j) + (J'_j - J''_j) R_j^+ \right] \left[1 + \frac{\delta^2}{2} \right] \quad (89)$$

$A(^3P_2) : \lambda = \pm 1$

$$- 4 v \lambda g_2^2 \frac{J'_j + J''_j}{P_j^2} \bar{\beta}_f^2 + \frac{4 v \bar{\beta}_f}{P_j^2} g_2^2 \left[(K'_j + K''_j) \frac{\delta^2}{2} - R_j^+ (K'_j - K''_j) \right] \quad (90)$$

$\lambda = 0$

$$\frac{8 v \bar{\beta}_f g_2^2}{\sqrt{3} R_W P_j^2} \left[\left[-1 + \Delta^2 + \frac{\delta^2}{2} \right] (K'_j + K''_j) - R_j^+ \left[1 + \frac{\delta^2}{2} \right] (K'_j - K''_j) \right] \quad (91)$$

In [34] the following definition is used:

$$\delta^2 = (R_W^2 - R_{H^+}^2)/2. \quad (92)$$

The couplings appearing in the chargino $\tilde{\chi}_j^+$ exchange are combined to:

$$J'_j = -\frac{1}{4} (O_{0j}^R - O_{0j}^L) (Q_{0j}'^R \sin \beta + Q_{0j}'^L \cos \beta) \quad (93)$$

$$J''_j = -\frac{1}{4} (O_{0j}^R + O_{0j}^L) (Q_{0j}'^R \sin \beta - Q_{0j}'^L \cos \beta) \quad (94)$$

$$K'_j = -\frac{1}{4} (O_{0j}^R - O_{0j}^L) (Q_{0j}'^R \sin \beta - Q_{0j}'^L \cos \beta) \quad (95)$$

$$K''_j = -\frac{1}{4} (O_{0j}^R + O_{0j}^L) (Q_{0j}'^R \sin \beta + Q_{0j}'^L \cos \beta). \quad (96)$$

L_i is the product of the coupling of the scalar Higgs S_i to the LSP neutralinos and to the W boson and the charged Higgs. In the NMSSM L_i is given by:

$$L_i = \frac{1}{2} (U_{i2}^S \cos \beta - U_{i1}^S \sin \beta) T_{S_i 00}. \quad (97)$$

In the NMSSM the coupling $g_{\alpha-+}$ of the pseudoscalar Higgs P_α to the W boson and charged Higgs reads:

$$g_{\alpha-+} = U_{\alpha 2}^P \cos \beta + U_{\alpha 1}^P \sin \beta. \quad (98)$$

In the MSSM with only one pseudoscalar Higgs P the coupling $g_{\alpha-+}$ turns out to be 1 [34].

$$6. \quad \tilde{\chi}_1^0 \tilde{\chi}_1^0 \rightarrow S_a S_b \text{ or } P_\alpha P_\beta.$$

The scalar Higgses S_a and S_b are produced by scalar Higgs S_i ($i = 1, 2, 3$) exchange in the s-channel and neutralino $\tilde{\chi}_j^0$ ($j = 1 - 5$) exchange in the t- and u-channel.

$A(^3P_0)$:

$$\sqrt{6} v g_2^2 \left[g_{abi} T_{S_i 00} \frac{R_Z}{4 - R_{S_i}^2 + iG_{S_i}} - 2 T_{S_a 0j} T_{S_b 0j} \frac{1 + R_j}{P_j} + \frac{4}{3} T_{S_a 0j} T_{S_b 0j} \frac{\bar{\beta}_f^2}{P_j^2} \right] \quad (99)$$

$A(^3P_2)$:

$$- \frac{8}{\sqrt{3}} v \bar{\beta}_f^2 g_2^2 T_{S_a 0j} T_{S_b 0j} \frac{1}{P_j^2} \quad (100)$$

The pseudoscalar Higgses P_α and P_β are also produced by scalar Higgs S_i ($i = 1, 2, 3$) exchange and neutralino $\tilde{\chi}_j^0$ ($j = 1 - 5$) exchange. The corresponding amplitudes for P_α and P_β production can be obtained by replacing a, b by α, β or S_a, S_b by P_α, P_β and R_j by $-R_j$. In the NMSSM the trilinear scalar Higgs coupling g_{aaa} is given by:

$$\begin{aligned} g_{aaa} = & -\frac{6}{g_2 m_Z} \left(\frac{g_y^2 + g_2^2}{8} \sqrt{2} (v_1 U_{a1}^{S3} + v_2 U_{a2}^{S3} - v_1 U_{a1}^S U_{a2}^{S2} - v_2 U_{a2}^S U_{a1}^{S2}) \right. \\ & + \frac{\lambda^2}{\sqrt{2}} v_2 U_{a2}^S U_{a3}^{S2} + \frac{\lambda^2}{\sqrt{2}} x U_{a3}^S U_{a2}^{S2} + \frac{\lambda^2}{\sqrt{2}} v_1 U_{a1}^S U_{a3}^{S2} + \frac{\lambda^2}{\sqrt{2}} x U_{a3}^S U_{a1}^{S2} \\ & + \frac{\lambda^2}{\sqrt{2}} v_1 U_{a1}^S U_{a2}^{S2} + \frac{\lambda^2}{\sqrt{2}} v_2 U_{a2}^S U_{a1}^{S2} + \sqrt{2} k^2 x U_{a3}^{S3} \\ & - \frac{\lambda k}{\sqrt{2}} v_1 U_{a2}^S U_{a3}^{S2} - \frac{\lambda k}{\sqrt{2}} v_2 U_{a1}^S U_{a3}^{S2} - \sqrt{2} \lambda k x U_{a1}^S U_{a2}^S U_{a3}^S \\ & \left. - \frac{\lambda A_\lambda}{\sqrt{2}} U_{a1}^S U_{a2}^S U_{a3}^S - \frac{k A_k}{3 \sqrt{2}} U_{a3}^{S3} \right). \quad (101) \end{aligned}$$

The trilinear scalar Higgs coupling g_{aab} (or g_{aba}) has the following form:

$$\begin{aligned} g_{aab} = g_{aba} = & -\frac{2}{g_2 m_Z} \left(\frac{g_y^2 + g_2^2}{8} \sqrt{2} (3 v_1 U_{b1}^S U_{a1}^{S2} + 3 v_2 U_{b2}^S U_{a2}^{S2} - v_1 U_{b1}^S U_{a2}^{S2} \right. \\ & \left. - 2 v_1 U_{a1}^S U_{b2}^S U_{a2}^S - v_2 U_{b2}^S U_{a1}^{S2} - 2 v_2 U_{a2}^S U_{b1}^S U_{a1}^S) \right) \end{aligned}$$

$$\begin{aligned}
& + \frac{\lambda^2 v_2 - \lambda k v_1}{\sqrt{2}} (U_{b2}^S U_{a3}^{S2} + 2 U_{a2}^S U_{b3}^S U_{a3}^S) + \frac{\lambda^2 x}{\sqrt{2}} (U_{b3}^S U_{a2}^{S2} + 2 U_{a3}^S U_{b2}^S U_{a2}^S) \\
& + \frac{\lambda^2 v_1 - \lambda k v_2}{\sqrt{2}} (U_{b1}^S U_{a3}^{S2} + 2 U_{a1}^S U_{b3}^S U_{a3}^S) + \frac{\lambda^2 x}{\sqrt{2}} (U_{b3}^S U_{a1}^{S2} + 2 U_{a3}^S U_{b1}^S U_{a1}^S) \\
& + \frac{\lambda^2 v_1}{\sqrt{2}} (U_{b1}^S U_{a2}^{S2} + 2 U_{a1}^S U_{b2}^S U_{a2}^S) + \frac{\lambda^2 v_2}{\sqrt{2}} (U_{b2}^S U_{a1}^{S2} + 2 U_{a2}^S U_{b1}^S U_{a1}^S) \\
& \quad + \frac{6 k^2 x - k A_k}{\sqrt{2}} U_{b3}^S U_{a3}^{S2} \\
& - \frac{2 \lambda k x + \lambda A_\lambda}{\sqrt{2}} (U_{b1}^S U_{a2}^S U_{a3}^S + U_{a1}^S U_{b2}^S U_{a3}^S + U_{a1}^S U_{a2}^S U_{b3}^S) \Big). \tag{102}
\end{aligned}$$

Finally the trilinear scalar Higgs coupling g_{123} (or g_{132} or g_{231}) reads:

$$\begin{aligned}
g_{123} = g_{132} = g_{231} = & - \frac{1}{g_2 m_Z} \left(\frac{g_y^2 + g_2^2}{8} \sqrt{2} (6 v_1 U_{11}^S U_{21}^S U_{31}^S + 6 v_2 U_{12}^S U_{22}^S U_{32}^S \right. \\
& - 2 v_1 (U_{11}^S U_{22}^S U_{32}^S + U_{21}^S U_{12}^S U_{32}^S + U_{31}^S U_{12}^S U_{22}^S) \\
& - 2 v_2 (U_{12}^S U_{21}^S U_{31}^S + U_{22}^S U_{11}^S U_{31}^S + U_{32}^S U_{11}^S U_{21}^S)) \\
& + \sqrt{2} (\lambda^2 v_2 - \lambda k v_1) (U_{12}^S U_{23}^S U_{33}^S + U_{22}^S U_{13}^S U_{33}^S + U_{32}^S U_{13}^S U_{23}^S) \\
& + \sqrt{2} \lambda^2 x (U_{13}^S U_{22}^S U_{32}^S + U_{23}^S U_{12}^S U_{32}^S + U_{33}^S U_{12}^S U_{22}^S) \\
& + \sqrt{2} (\lambda^2 v_1 - \lambda k v_2) (U_{11}^S U_{23}^S U_{33}^S + U_{21}^S U_{13}^S U_{33}^S + U_{31}^S U_{13}^S U_{23}^S) \\
& + \sqrt{2} \lambda^2 x (U_{13}^S U_{21}^S U_{31}^S + U_{23}^S U_{11}^S U_{31}^S + U_{33}^S U_{11}^S U_{21}^S) \\
& + \sqrt{2} \lambda^2 v_1 (U_{11}^S U_{22}^S U_{32}^S + U_{21}^S U_{12}^S U_{32}^S + U_{31}^S U_{12}^S U_{22}^S) \\
& + \sqrt{2} \lambda^2 v_2 (U_{12}^S U_{21}^S U_{31}^S + U_{22}^S U_{11}^S U_{31}^S + U_{32}^S U_{11}^S U_{21}^S) \\
& \quad + \sqrt{2} (6 k^2 x - k A_k) U_{13}^S U_{23}^S U_{33}^S \\
& - \frac{2 \lambda k x + \lambda A_\lambda}{\sqrt{2}} (U_{11}^S U_{22}^S U_{33}^S + U_{11}^S U_{32}^S U_{23}^S + U_{21}^S U_{12}^S U_{33}^S \\
& \quad + U_{21}^S U_{32}^S U_{13}^S + U_{31}^S U_{12}^S U_{23}^S + U_{31}^S U_{22}^S U_{13}^S) \Big). \tag{103}
\end{aligned}$$

The trilinear scalar and pseudoscalar Higgs coupling $g_{\alpha\alpha\alpha}$ (or $g_{a\alpha\alpha}$) is given by:

$$g_{\alpha\alpha\alpha} = g_{a\alpha\alpha} = - \frac{2}{g_2 m_Z} \left(\frac{g_y^2 + g_2^2}{8} \sqrt{2} (v_1 U_{a1}^S U_{a1}^{P2} + v_2 U_{a2}^S U_{a2}^{P2} \right.$$

$$\begin{aligned}
& -v_1 U_{a1}^S U_{a2}^{P2} - v_2 U_{a2}^S U_{a1}^{P2}) + \frac{\lambda^2}{\sqrt{2}} (v_2 U_{a2}^S U_{a3}^{P2} + x U_{a3}^S U_{a2}^{P2} + v_1 U_{a1}^S U_{a3}^{P2} \\
& \quad + x U_{a3}^S U_{a1}^{P2} + v_1 U_{a1}^S U_{a2}^{P2} + v_2 U_{a2}^S U_{a1}^{P2}) \\
& \quad + \sqrt{2} k^2 x U_{a3}^S U_{a3}^{P2} + \frac{\lambda k}{\sqrt{2}} (v_1 U_{a2}^S U_{a3}^{P2} + v_2 U_{a1}^S U_{a3}^{P2}) \\
& \quad - \sqrt{2} \lambda k (v_1 U_{a3}^S U_{a3}^P U_{a2}^P + v_2 U_{a3}^S U_{a3}^P U_{a1}^P \\
& \quad + x U_{a1}^S U_{a2}^P U_{a3}^P + x U_{a2}^S U_{a1}^P U_{a3}^P - x U_{a3}^S U_{a1}^P U_{a2}^P) \\
& \quad + \frac{\lambda A_\lambda}{\sqrt{2}} (U_{a1}^S U_{a2}^P U_{a3}^P + U_{a2}^S U_{a1}^P U_{a3}^P + U_{a3}^S U_{a1}^P U_{a2}^P) + \frac{k A_k}{\sqrt{2}} U_{a3}^S U_{a3}^{P2}). \tag{104}
\end{aligned}$$

The trilinear scalar and pseudoscalar Higgs coupling $g_{\alpha\beta a}$ (or $g_{a\alpha\beta}$ or $g_{a\beta\alpha}$) can be written as:

$$\begin{aligned}
g_{\alpha\beta a} = g_{a\alpha\beta} = g_{a\beta\alpha} = & -\frac{1}{g_2 m_Z} \left(\frac{g_y^2 + g_2^2}{8} \sqrt{2} (v_1 U_{a1}^S U_{a1}^P U_{\beta 1}^P \right. \\
& + v_2 U_{a2}^S U_{a2}^P U_{\beta 2}^P - v_1 U_{a1}^S U_{a2}^P U_{\beta 2}^P - v_2 U_{a2}^S U_{a1}^P U_{\beta 1}^P) \\
& + \sqrt{2} \lambda^2 (v_2 U_{a2}^S U_{a3}^P U_{\beta 3}^P + x U_{a3}^S U_{a2}^P U_{\beta 2}^P + v_1 U_{a1}^S U_{a3}^P U_{\beta 3}^P \\
& + x U_{a3}^S U_{a1}^P U_{\beta 1}^P + v_1 U_{a1}^S U_{a2}^P U_{\beta 2}^P + v_2 U_{a2}^S U_{a1}^P U_{\beta 1}^P) + 2 \sqrt{2} k^2 x U_{a3}^S U_{a3}^P U_{\beta 3}^P \\
& + \sqrt{2} \lambda k v_1 U_{a2}^S U_{a3}^P U_{\beta 3}^P - \sqrt{2} \lambda k v_1 U_{a3}^S (U_{a3}^P U_{\beta 2}^P + U_{\beta 3}^P U_{a2}^P) \\
& + \sqrt{2} \lambda k v_2 U_{a1}^S U_{a3}^P U_{\beta 3}^P - \sqrt{2} \lambda k v_2 U_{a3}^S (U_{a3}^P U_{\beta 1}^P + U_{\beta 3}^P U_{a1}^P) \\
& \left. + \frac{-2 \lambda k x + \lambda A_\lambda}{\sqrt{2}} (U_{a1}^S (U_{a2}^P U_{\beta 3}^P + U_{\beta 2}^P U_{a3}^P) + U_{a2}^S (U_{a1}^P U_{\beta 3}^P + U_{\beta 1}^P U_{a3}^P)) \right) \\
& + \frac{2 \lambda k x + \lambda A_\lambda}{\sqrt{2}} U_{a3}^S (U_{a1}^P U_{\beta 2}^P + U_{\beta 1}^P U_{a2}^P) + \sqrt{2} k A_k U_{a3}^S U_{a3}^P U_{\beta 3}^P). \tag{105}
\end{aligned}$$

$$7. \tilde{\chi}_1^0 \tilde{\chi}_1^0 \rightarrow S_a P_\beta.$$

The scalar Higgs S_a and the pseudoscalar Higgs P_β are produced by Z boson and pseudoscalar Higgs P_α ($\alpha = 1, 2$) exchange in the s-channel and neutralino $\tilde{\chi}_j^0$ ($j = 1 - 5$) exchange in the t- and u-channel.

$A(^1S_0)$:

$$2 \sqrt{2} g_2^2 g_{a\alpha\beta} T_{P_\alpha 00} \frac{R_Z}{4 - R_{P_\alpha}^2} \left[1 + \frac{v^2}{8} \right] + \sqrt{2} g_2^2 g_{a\beta Z} \frac{R_{P_\beta}^2 - R_{S_a}^2}{R_Z^2} \left[1 - \frac{v^2}{8} \right]$$

$$\begin{aligned}
& -4\sqrt{2}g_2^2 T_{S_a 0j} T_{P_\beta 0j} \frac{R_j}{P_j} \left[1 + v^2 \left[\frac{1}{8} - \frac{1}{2P_j} + \frac{\bar{\beta}_f^2}{3P_j^2} \right] \right] \\
& - \sqrt{2} (R_{P_\beta}^2 - R_{S_a}^2) g_2^2 T_{S_a 0j} T_{P_\beta 0j} \left[1 + v^2 \left[-\frac{1}{8} - \frac{1}{2P_j} + \frac{\bar{\beta}_f^2}{3P_j^2} \right] \right]
\end{aligned} \tag{106}$$

$A(^3P_1)$:

$$-4v\bar{\beta}_f \frac{g_2^2 g_{a\beta Z}}{4 - R_Z^2 + iG_Z} - 4v\bar{\beta}_f g_2^2 \frac{T_{S_a 0j} T_{P_\beta 0j}}{P_j} \tag{107}$$

$G_Z = \Gamma_Z m_Z / m_{\tilde{\chi}}^2$ is the rescaled widths of the Z boson. The couplings appearing in the Z boson exchange are combined to $g_{a\beta Z}$. In the NMSSM $g_{a\beta Z}$ has the following form:

$$g_{a\beta Z} = -\frac{1}{2 \cos^2 \theta_W} (U_{a2}^S U_{\beta 2}^P - U_{a1}^S U_{\beta 1}^P) O_{00}^{\prime L}. \tag{108}$$

$$8. \quad \tilde{\chi}_1^0 \tilde{\chi}_1^0 \rightarrow H^+ H^-.$$

The charged Higgses are produced by Z boson and scalar Higgs S_i ($i = 1, 2, 3$) exchange in the s-channel and chargino $\tilde{\chi}_j^\pm$ ($j = 1, 2$) exchange in the t- and u-channel.

$A(^3P_0)$:

$$\begin{aligned}
& -\sqrt{6}v g_2^2 \left[(Q_{0j}^{\prime L2} + Q_{0j}^{\prime R2}) \left[\frac{1}{P_j} - \frac{2\bar{\beta}_f^2}{3P_j^2} \right] + 2Q_{0j}^{\prime L} Q_{0j}^{\prime R} \frac{R_j^+}{P_j} \right] \\
& + \sqrt{6}v g_2^2 R_W \frac{g_{+-i}}{4 - R_{S_i}^2}
\end{aligned} \tag{109}$$

$A(^3P_1)$:

$$2v\bar{\beta}_f g_2^2 (Q_{0j}^{\prime L2} - Q_{0j}^{\prime R2}) \frac{1}{P_j} + 4v\bar{\beta}_f \frac{\cos(2\theta_W)}{\cos^2 \theta_W} g_2^2 \frac{O_{00}^{\prime L}}{4 - R_Z^2} \tag{110}$$

$A(^3P_2)$:

$$\frac{4}{\sqrt{3}} v \bar{\beta}_f^2 g_2^2 (Q_{0j}^{\prime L2} + Q_{0j}^{\prime R2}) \frac{1}{P_j^2} \tag{111}$$

g_{+-i} is the product of the coupling of the scalar Higgs S_i to the LSP neutralinos and to the charged Higgses. In the NMSSM g_{+-i} is given by:

$$\begin{aligned}
g_{+-i} = & -T_{S_i 00} \left[(U_{i2}^S \sin \beta + U_{i1}^S \cos \beta) + \frac{\cos(2\beta)}{2 \cos^2 \theta_W} (-U_{i1}^S \cos \beta + U_{i2}^S \sin \beta) \right. \\
& - \frac{\sqrt{2} \lambda^2 v}{g_2 m_W} (U_{i2}^S \sin \beta \cos^2 \beta + U_{i1}^S \sin^2 \beta \cos \beta) + \frac{\sqrt{2} \lambda^2 x}{g_2 m_W} U_{i3}^S \\
& \left. + \frac{2 \sqrt{2} \lambda k x}{g_2 m_W} U_{i3}^S \sin \beta \cos \beta + \frac{\sqrt{2} \lambda A_\lambda}{g_2 m_W} U_{i3}^S \sin \beta \cos \beta \right]. \tag{112}
\end{aligned}$$

$$9. \quad \tilde{\chi}_1^0 \tilde{\chi}_1^0 \rightarrow f_a(h) \bar{f}_a(\bar{h}).$$

The fermions are produced by Z boson, scalar Higgs S_i ($i = 1, 2, 3$) and pseudoscalar Higgs P_α ($\alpha = 1, 2$) exchange in the s-channel and sfermion $\tilde{f}_{1,2}$ exchange in the t- and u-channel.

$$A(^1S_0) : \lambda_f = 0$$

$$\begin{aligned}
& \sqrt{2} (-1)^{\bar{h}+1/2} (X'_{a0}{}^2 + W'_{a0}{}^2) \left[1 + v^2 \left[-\frac{1}{2P_1} + \frac{\bar{\beta}_f^2}{3P_1^2} \right] \right] \frac{R_f}{P_1} \\
& + 2 \sqrt{2} (-1)^{\bar{h}+1/2} X'_{a0} W'_{a0} \frac{1}{P_1} \left[1 + v^2 \left[\frac{1}{4} - \frac{1}{2P_1} - \frac{\bar{\beta}_f^2}{6P_1} + \frac{\bar{\beta}_f^2}{3P_1^2} \right] \right] \\
& + (X'_{a0} \leftrightarrow Z'_{a0}, W'_{a0} \leftrightarrow Y'_{a0}, P_1 \leftrightarrow P_2) + (-1)^{\bar{h}+1/2} \frac{2 \sqrt{2} g_2^2}{\cos^2 \theta_W} O''_{00} T_{3a} \frac{R_f}{R_Z^2} \\
& + 4 \sqrt{2} (-1)^{\bar{h}+1/2} g_2 h_{P_\alpha a} T_{P_\alpha 00} \frac{1}{4 - R_{P_\alpha}^2 + iG_{P_\alpha}} \left[1 + \frac{v^2}{4} \right] \tag{113}
\end{aligned}$$

$$A(^3P_0) : \lambda_f = 0$$

$$\begin{aligned}
& -\sqrt{6} v \bar{\beta}_f (X'_{a0} W'_{a0}) \left[\frac{1}{P_1} - \frac{2}{3P_1^2} \right] + \frac{\sqrt{6}}{3} v \bar{\beta}_f (X'_{a0}{}^2 + W'_{a0}{}^2) \frac{R_f}{P_1^2} \\
& + (X'_{a0} \leftrightarrow Z'_{a0}, W'_{a0} \leftrightarrow Y'_{a0}, P_1 \leftrightarrow P_2) - 2 \sqrt{6} v \bar{\beta}_f g_2 \frac{h_{S_i a} T_{S_i 00}}{4 - R_{S_i}^2 + iG_{S_i}} \tag{114}
\end{aligned}$$

$A(^3P_1) : \lambda_f = 0$

$$\begin{aligned} & \frac{v R_f}{P_1} (X'_{a0}{}^2 - W'_{a0}{}^2) + (X'_{a0} \leftrightarrow Z'_{a0}, W'_{a0} \leftrightarrow Y'_{a0}, P_1 \leftrightarrow P_2) \\ & - 2 v g_2^2 \frac{O''_{00}{}^L}{\cos^2 \theta_W} [T_{3a} - 2 e_{f_a} \sin^2 \theta_W] \frac{R_f}{4 - R_Z^2 + iG_Z} \end{aligned} \quad (115)$$

$\lambda_f = \pm 1$

$$\begin{aligned} & \sqrt{2} v \left[\lambda_f \bar{\beta}_f (X'_{a0}{}^2 + W'_{a0}{}^2) \left[-\frac{1}{P_1} + \frac{1}{P_1^2} \right] + (X'_{a0}{}^2 - W'_{a0}{}^2) \left[\frac{1}{P_1} - \frac{\bar{\beta}_f^2}{P_1^2} \right] \right. \\ & \left. + 2 \bar{\beta}_f \lambda_f X'_{a0} W'_{a0} \frac{R_f}{P_1^2} \right] + (X'_{a0} \leftrightarrow Z'_{a0}, W'_{a0} \leftrightarrow Y'_{a0}, P_1 \leftrightarrow P_2) \\ & + 2 \sqrt{2} v \frac{g_2^2}{\cos^2 \theta_W} O''_{00}{}^L [\lambda_f T_{3a} \bar{\beta}_f - (T_{3a} - 2 e_{f_a} \sin^2 \theta_W)] \frac{1}{4 - R_Z^2 + iG_Z} \end{aligned} \quad (116)$$

$A(^3P_2) : \lambda_f = 0$

$$\begin{aligned} & -\frac{2}{\sqrt{3}} v \bar{\beta}_f \frac{1}{P_1^2} \left[R_f (X'_{a0}{}^2 + W'_{a0}{}^2) + 2 X'_{a0} W'_{a0} \right] \\ & + (X'_{a0} \leftrightarrow Z'_{a0}, W'_{a0} \leftrightarrow Y'_{a0}, P_1 \leftrightarrow P_2) \end{aligned} \quad (117)$$

$\lambda_f = \pm 1$

$$\begin{aligned} & \sqrt{2} v \bar{\beta}_f \frac{1}{P_1^2} [-(X'_{a0}{}^2 + W'_{a0}{}^2) + \bar{\beta}_f \lambda_f (X'_{a0}{}^2 - W'_{a0}{}^2) - 2 R_f X'_{a0} W'_{a0}] \\ & + (X'_{a0} \leftrightarrow Z'_{a0}, W'_{a0} \leftrightarrow Y'_{a0}, P_1 \leftrightarrow P_2). \end{aligned} \quad (118)$$

The sfermion mass eigenstates $\tilde{f}_{1,2}$ are defined by

$$\tilde{f}_1 = \tilde{f}_L \cos \theta_f + \tilde{f}_R \sin \theta_f \quad (119)$$

$$\tilde{f}_2 = -\tilde{f}_L \sin \theta_f + \tilde{f}_R \cos \theta_f. \quad (120)$$

The couplings of the mixed sfermion $\tilde{f}_{1,2}$ to the fermion and LSP neutralino can be written as:

$$X'_{a0} = X_{a0} \cos \theta_f + Z_{a0} \sin \theta_f \quad (121)$$

$$W'_{a0} = Z_{a0} \cos \theta_f + Y_{a0} \sin \theta_f \quad (122)$$

$$Z'_{a0} = -X_{a0} \sin \theta_f + Z_{a0} \cos \theta_f \quad (123)$$

$$Y'_{a0} = -Z_{a0} \sin \theta_f + Y_{a0} \cos \theta_f, \quad (124)$$

where the couplings of the unmixed sfermion $\tilde{f}_{L,R}$ to the fermion and LSP neutralino are given by:

$$X_{a0} = -\sqrt{2} g_2 [T_{3a} N_{02} - \tan \theta_W (T_{3a} - e_{f_a}) N_{01}] \quad (125)$$

$$Y_{a0} = \sqrt{2} g_2 \tan \theta_W e_{f_a} N_{01} \quad (126)$$

$$Z_{u0} = -\frac{g_2 m_u}{\sqrt{2} \sin \beta m_W} N_{04} \quad (127)$$

$$Z_{d0} = -\frac{g_2 m_d}{\sqrt{2} \cos \beta m_W} N_{03}. \quad (128)$$

In the NMSSM the couplings of the Higgses to the fermions have to be modified compared to the MSSM:

$$h_{S_i u} = -\frac{g_2 m_u U_{i2}^S}{2 \sin \beta m_W} \quad h_{S_i d} = -\frac{g_2 m_d U_{i1}^S}{2 \cos \beta m_W} \quad (129)$$

$$h_{P_\alpha u} = -\frac{g_2 m_u U_{\alpha 2}^P}{2 \sin \beta m_W} \quad h_{P_\alpha d} = -\frac{g_2 m_d U_{\alpha 1}^P}{2 \cos \beta m_W}. \quad (130)$$

Appendix A2: Renormalisation Group Equations

For completeness we also give here the 1 loop SUSY RGEs [18] for the parameters in the NMSSM with our conventions. Q is the running mass scale in the variable $t = \log(Q/M_{weak})$.

$$\frac{d}{dt} g_y = \frac{11}{16 \pi^2} g_y^3 \quad (131)$$

$$\frac{d}{dt} g_2 = \frac{1}{16 \pi^2} g_2^3 \quad (132)$$

$$\frac{d}{dt} g_3 = -\frac{3}{16 \pi^2} g_3^3 \quad (133)$$

$$\frac{d}{dt} \lambda = \frac{1}{8 \pi^2} \left(k^2 + 2 \lambda^2 + \frac{3}{2} h_t^2 - \frac{3}{2} g_2^2 - \frac{1}{2} g_y^2 \right) \lambda \quad (134)$$

$$\frac{d}{dt} k = \frac{3}{8 \pi^2} (k^2 + \lambda^2) k \quad (135)$$

$$\frac{d}{dt} h_t = \frac{1}{8 \pi^2} \left(\frac{1}{2} \lambda^2 + 3 h_t^2 - \frac{8}{3} g_3^2 - \frac{3}{2} g_2^2 - \frac{13}{18} g_y^2 \right) h_t \quad (136)$$

$$\begin{aligned} \frac{d}{dt} A_\lambda &= \frac{1}{8 \pi^2} (4 \lambda^2 A_\lambda - 2 k^2 A_k - 3 h_t^2 A_{U_3} \\ &\quad - 3 g_2^2 M_2 - g_y^2 M_1) \end{aligned} \quad (137)$$

$$\frac{d}{dt} A_k = \frac{6}{8 \pi^2} (-\lambda^2 A_\lambda + k^2 A_k) \quad (138)$$

$$\begin{aligned} \frac{d}{dt} A_{U_i} &= \frac{1}{8 \pi^2} \left(-\lambda^2 A_\lambda + 3(1 + \delta_{i3}) h_t^2 A_{U_3} \right. \\ &\quad \left. + \frac{16}{3} g_3^2 M_3 + 3 g_2^2 M_2 + \frac{13}{9} g_y^2 M_1 \right) \end{aligned} \quad (139)$$

$$\begin{aligned} \frac{d}{dt} A_{D_i} &= \frac{1}{8 \pi^2} \left(-\lambda^2 A_\lambda + \delta_{i3} h_t^2 A_{U_3} \right. \\ &\quad \left. + \frac{16}{3} g_3^2 M_3 + 3 g_2^2 M_2 + \frac{7}{9} g_y^2 M_1 \right) \end{aligned} \quad (140)$$

$$\frac{d}{dt} A_{E_i} = \frac{1}{8 \pi^2} (-\lambda^2 A_\lambda + 3 g_2^2 M_2 + 3 g_y^2 M_1) \quad (141)$$

$$\begin{aligned} \frac{d}{dt} m_N^2 &= \frac{1}{8 \pi^2} [2 \lambda^2 (m_N^2 + m_{H_1}^2 + m_{H_2}^2 + A_\lambda^2) \\ &\quad + 2 k^2 (3 m_N^2 + A_k^2)] \end{aligned} \quad (142)$$

$$\begin{aligned} \frac{d}{dt} m_{H_1}^2 &= \frac{1}{8 \pi^2} [\lambda^2 (m_N^2 + m_{H_1}^2 + m_{H_2}^2 + A_\lambda^2) \\ &\quad - 3 g_2^2 M_2^2 - g_y^2 M_1^2] \end{aligned} \quad (143)$$

$$\frac{d}{dt} m_{H_2}^2 = \frac{d}{dt} m_{H_1}^2 + \frac{3}{8 \pi^2} h_t^2 (m_{H_2}^2 + m_{U_3}^2 + m_{Q_3}^2 + A_{U_3}^2) \quad (144)$$

$$\begin{aligned} \frac{d}{dt} m_{Q_i}^2 &= \frac{1}{8 \pi^2} \left[\delta_{i3} h_t^2 (m_{H_2}^2 + m_{U_3}^2 + m_{Q_3}^2 + A_{U_3}^2) \right. \\ &\quad \left. - \frac{16}{3} g_3^2 M_3^2 - 3 g_2^2 M_2^2 - \frac{1}{9} g_y^2 M_1^2 \right] \end{aligned} \quad (145)$$

$$\begin{aligned} \frac{d}{dt} m_{U_i}^2 &= \frac{1}{8 \pi^2} \left[2 \delta_{i3} h_t^2 (m_{H_2}^2 + m_{U_3}^2 + m_{Q_3}^2 + A_{U_3}^2) \right. \\ &\quad \left. - \frac{16}{3} g_3^2 M_3^2 - \frac{16}{9} g_y^2 M_1^2 \right] \end{aligned} \quad (146)$$

$$\frac{d}{dt} m_{D_i}^2 = \frac{1}{8 \pi^2} \left(-\frac{16}{3} g_3^2 M_3^2 - \frac{4}{9} g_y^2 M_1^2 \right) \quad (147)$$

$$\frac{d}{dt} m_{L_i}^2 = \frac{1}{8 \pi^2} (-3 g_2^2 M_2^2 - g_y^2 M_1^2) \quad (148)$$

$$\frac{d}{dt} m_{E_i}^2 = \frac{1}{8 \pi^2} (-4 g_y^2 M_1^2) \quad (149)$$

$$\frac{d}{dt} M_1 = \frac{11}{8 \pi^2} g_y^2 M_1 \quad (150)$$

$$\frac{d}{dt} M_2 = \frac{1}{8 \pi^2} g_2^2 M_2 \quad (151)$$

$$\frac{d}{dt} M_3 = -\frac{3}{8 \pi^2} g_3^2 M_3 \quad (152)$$

References

- [1] H.P. Nilles, Phys. Rep. 110 (1984) 1.
- [2] H.E. Haber, G.L. Kane, Phys. Rep. 117 (1985) 75;
J.F. Gunion, H.E. Haber, Nucl. Phys. B272 (1986) 1.
- [3] J. Ellis, J.F. Gunion, H.E. Haber, L. Roszkowski, F. Zwirner,
Phys. Rev. D39 (1989) 844.
- [4] S.A. Abel, S. Sarkar, P.L. White, Nucl. Phys. B454 (1995) 663;
S.A. Abel, Nucl. Phys. B480 (1996) 55.
- [5] U. Ellwanger, M. Rausch de Traubenberg, Z Phys. C53 (1992) 521.
- [6] U. Ellwanger, Phys. Lett. B303 (1993) 271.
- [7] U. Ellwanger, M. Rausch de Traubenberg, C.A. Savoy, Phys. Lett. B315 (1993) 331.
- [8] U. Ellwanger, M. Rausch de Traubenberg, C.A. Savoy, Z Phys. C67 (1995) 665.
- [9] U. Ellwanger, M. Rausch de Traubenberg, C.A. Savoy, Nucl. Phys. B492 (1997) 21.
- [10] U. Ellwanger, C. Hugonie, Laboratoire de Physique Théorique et Hautes Energies
Université de Paris-Sud, Orsay preprint LPTHE-97-68, hep-ph/9712300.
- [11] T. Elliott, S.F. King, P.L. White, Phys. Lett. B305 (1993) 71.
- [12] T. Elliott, S.F. King, P.L. White, Phys. Lett. B314 (1993) 56;
Phys. Rev. D49 (1994) 2435.
- [13] S.F. King, P.L. White, Phys. Rev. D52 (1995) 4183.
- [14] B. Ananthanarayan, P.N. Pandita, Phys. Lett. B371 (1996) 245.

- [15] F. Franke, H. Fraas, A. Bartl, Phys. Lett. B336 (1994) 415;
F. Franke, H. Fraas, Phys. Lett. B353 (1995) 234; Z Phys. C72 (1996) 309.
- [16] B.R. Greene, P.J. Miron, Phys. Lett. B168 (1986) 226;
R. Flores, K.A. Olive, D. Thomas, Phys. Lett. B245 (1990) 509;
K.A. Olive, D. Thomas, Nucl. Phys. B355 (1991) 192.
- [17] S.A. Abel, S. Sarkar, I.B. Whittingham, Nucl. Phys. B392 (1993) 83.
- [18] J.P. Derendinger, C.A. Savoy, Nucl. Phys. B237 (1984) 307.
- [19] J.A. Casas, A. Lleyda, C. Muñoz, Nucl. Phys. B471 (1996) 3;
J.A. Casas, Instituto de Estructura de la Materia, Madrid
preprint IEM-FT-161-97, hep-ph/9707475;
C. Muñoz, Departamento de Física Teórica, Universidad Autónoma de Madrid,
preprint FTUAM-97-20, hep-ph/9709329.
- [20] A. Stephan, Phys. Lett. B411 (1997) 97.
- [21] A. Bartl, H. Fraas, W. Majerotto, Nucl. Phys. B278 (1986) 1.
- [22] C. Giunti, C.W. Kim, U.W. Lee, Mod. Phys. Lett. A6 (1991) 1745;
J. Ellis, S. Kelley, D.V. Nanopoulos, Phys. Lett. B260 (1991) 131;
U. Amaldi, W. de Boer, H. Fürstenau, Phys. Lett. B260 (1991) 447;
P. Langacker, M. Luo, Phys. Rev. D44 (1991) 817.
- [23] M. Gallinaro, CDF Collab., preprint FERMILAB-CONF-97/004-E.
- [24] Particle Data Group, R.M. Barnett et al., Phys. Rev. D54 (1996) 1.
- [25] DELPHI Collab., P. Andersson et al., Search for Sfermions at $\sqrt{s} = 161$ and $172 GeV$,
contribution to the HEP'97 Conference Jerusalem, August 19-26, Ref.#353.
- [26] M. Bisset, S. Raychaudhuri, D.K. Ghosh, Tata Institute of Fundamental Research,
Mumbai preprint TIFR-TH-96-45, hep-ph/9608421.
- [27] CDF Collab., F. Abe et al., Phys. Rev. D56 (1997) R1357.

- [28] L3 Collab., M. Acciarri et al., Preliminary results on New Particle Searches at $\sqrt{s} = 183 \text{ GeV}$, contribution to the HEP'97 Conference Jerusalem, August 19-26, Ref.#859.
- [29] OPAL Collab., K. Ackerstaff et al., Search for charged Higgs bosons in e^+e^- collisions at $\sqrt{s} = 130 - 172 \text{ GeV}$, contribution to the HEP'97 Conference Jerusalem, August 19-26, Ref.#258.
- [30] ALEPH Collab., R. Barate et al., Preliminary ALEPH results at $\sqrt{s} = 183 \text{ GeV}$, contribution to the HEP'97 Conference Jerusalem, August 19-26, Ref.#856.
- [31] L3 Collab., M. Acciarri et al., Phys. Lett. B385 (1996) 454;
ALEPH Collab., R. Barate et al., preprint CERN-PPE/97-071,
submitted to Phys. Lett. B.
- [32] M.A. Diaz, S.F. King, Phys. Lett. B349 (1995) 105.
- [33] M. Davis, F. Summers, D. Schlegel, Nature 359 (1992) 393;
A. Klypin, J. Holtzman, J.R. Primack, E. Regös, Astrophys. J. 416 (1993) 1.
- [34] M. Drees, M.M. Nojiri, Phys. Rev. D47 (1993) 376.
- [35] M. Drees, Seoul National University, preprint APCTP-96-04, hep-ph/9609300.
- [36] E.W. Kolb, M.S. Turner, The Early Universe (Addison-Wesley, New York, 1990).
- [37] K. Griest, M. Kamionkowski, M.S. Turner, Phys. Rev. D41 (1990) 3565.
- [38] K. Griest, D. Seckel, Phys. Rev. D43 (1991) 3191;
P. Gondolo, G. Gelmini, Nucl. Phys. B360 (1991) 145;
P. Nath, R. Arnowitt, Phys. Rev. Lett. 70 (1993) 3696;
H. Baer, M. Brhlick, Phys. Rev. D53 (1996) 597.
- [39] J. Edsjö, P. Gondolo, Phys. Rev. D56 (1997) 1879.
- [40] A. Bartl, H. Fraas, W. Majerotto, B. Mösslacher, Z Phys. C55 (1992) 257.
- [41] G.L. Kane, C. Kolda, L. Roszkowski, J.D. Wells, Phys. Rev. D49 (1994) 6173.
- [42] C. Kolda, L. Roszkowski, J.D. Wells, G.L. Kane, Phys. Rev. D50 (1994) 3498.

[43] V. Barger, M.S. Berger, P. Ohmann, Phys. Rev. D49 (1994) 4908.

[44] M. Drees, private communication.

Figure Captions

Fig 1 The scalar mass m_0 versus the gaugino mass $|m_{1/2}|$. The upper pictures are for the MSSM, the lower pictures are for the NMSSM. In the right pictures the dark matter condition is imposed.

Fig 2 The trilinear coupling $|A_0|$ versus the scalar mass m_0 . The upper pictures are for the MSSM, the lower pictures are for the NMSSM. In the right pictures the dark matter condition is imposed.

Fig 3 The gaugino mass $|M_2|$ versus the Higgs mixing parameter μ both taken at the electroweak scale. The upper pictures are for the MSSM, the lower pictures are for the NMSSM. In the right pictures the dark matter condition is imposed.

Fig 4 The bino portion of the LSP neutralino versus the mass of the LSP neutralino. The upper pictures are for the MSSM, the lower pictures are for the NMSSM. In the right pictures the dark matter condition is imposed.

Fig 5 The mass of the lighter chargino versus the lighter selectron mass. The upper pictures are for the MSSM, the lower pictures are for the NMSSM. In the right pictures the dark matter condition is imposed.

Fig 6 The mass of the lighter u-squark versus the gluino mass. The upper pictures are for the MSSM, the lower pictures are for the NMSSM. In the right pictures the dark matter condition is imposed.

Fig 7 The mass of the lighter stop versus the gluino mass. The upper pictures are for the MSSM, the lower pictures are for the NMSSM. In the right pictures the dark matter condition is imposed.

Fig 8 The mass of the lightest scalar Higgs S_1 versus $|\tan\beta|$. The upper pictures are for the MSSM, the lower pictures are for the NMSSM. In the right pictures the dark matter condition is imposed.

Fig 9 The mass of the lightest scalar Higgs S_1 versus the mass of the lightest pseudoscalar Higgs P_1 . The upper pictures are for the MSSM, the lower pictures are for the NMSSM. In the right pictures the dark matter condition is imposed.

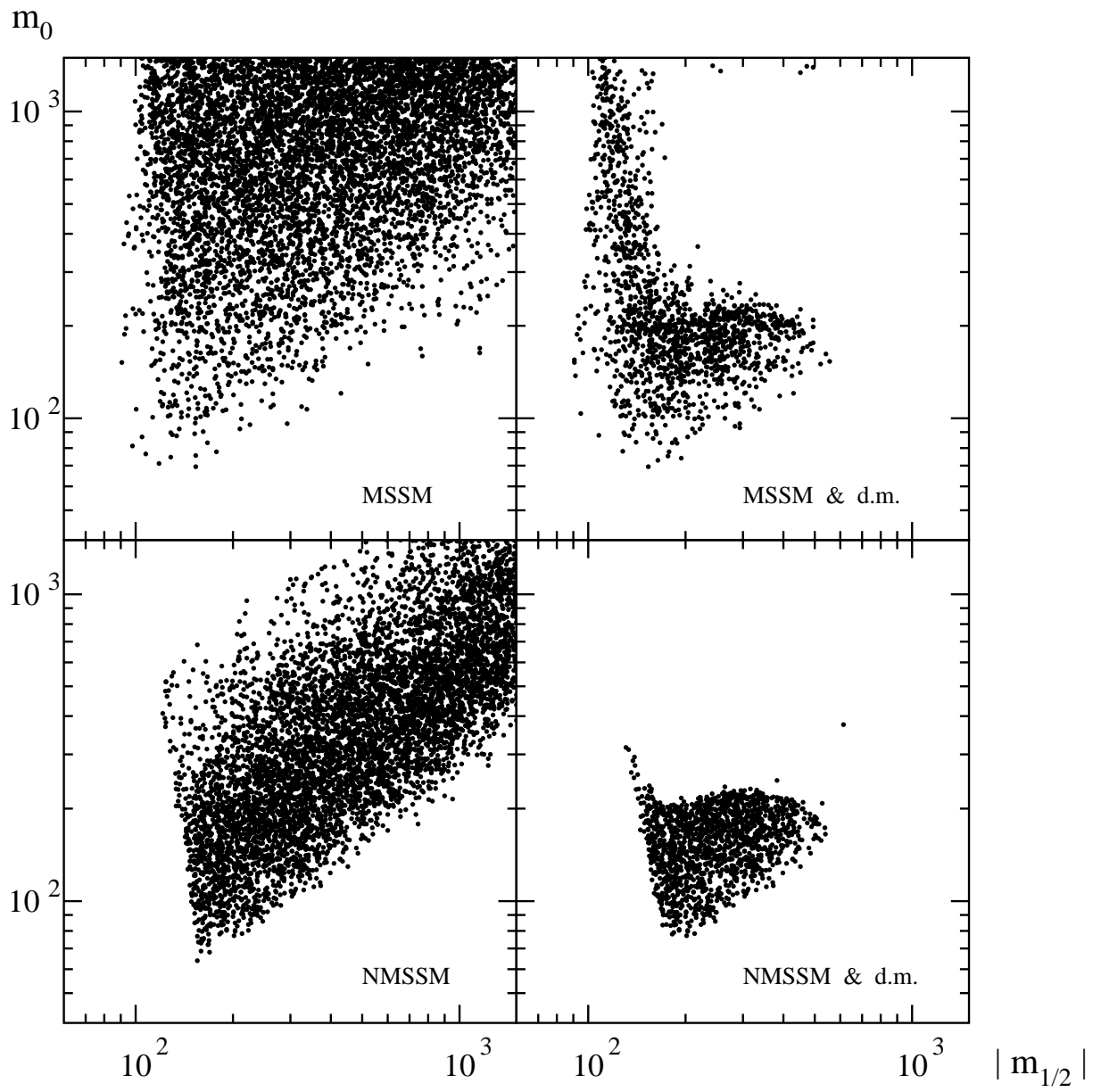


Fig. 1

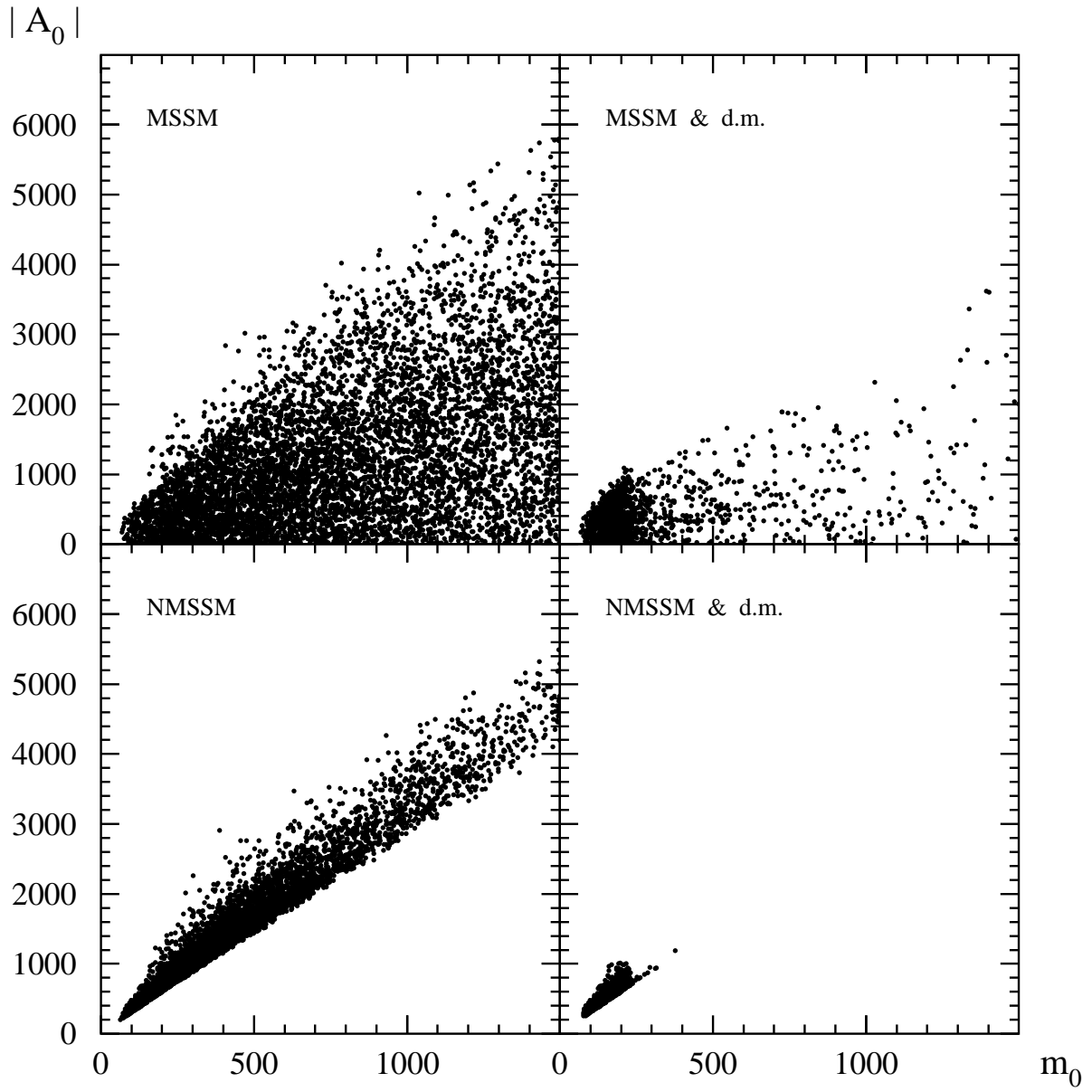


Fig. 2

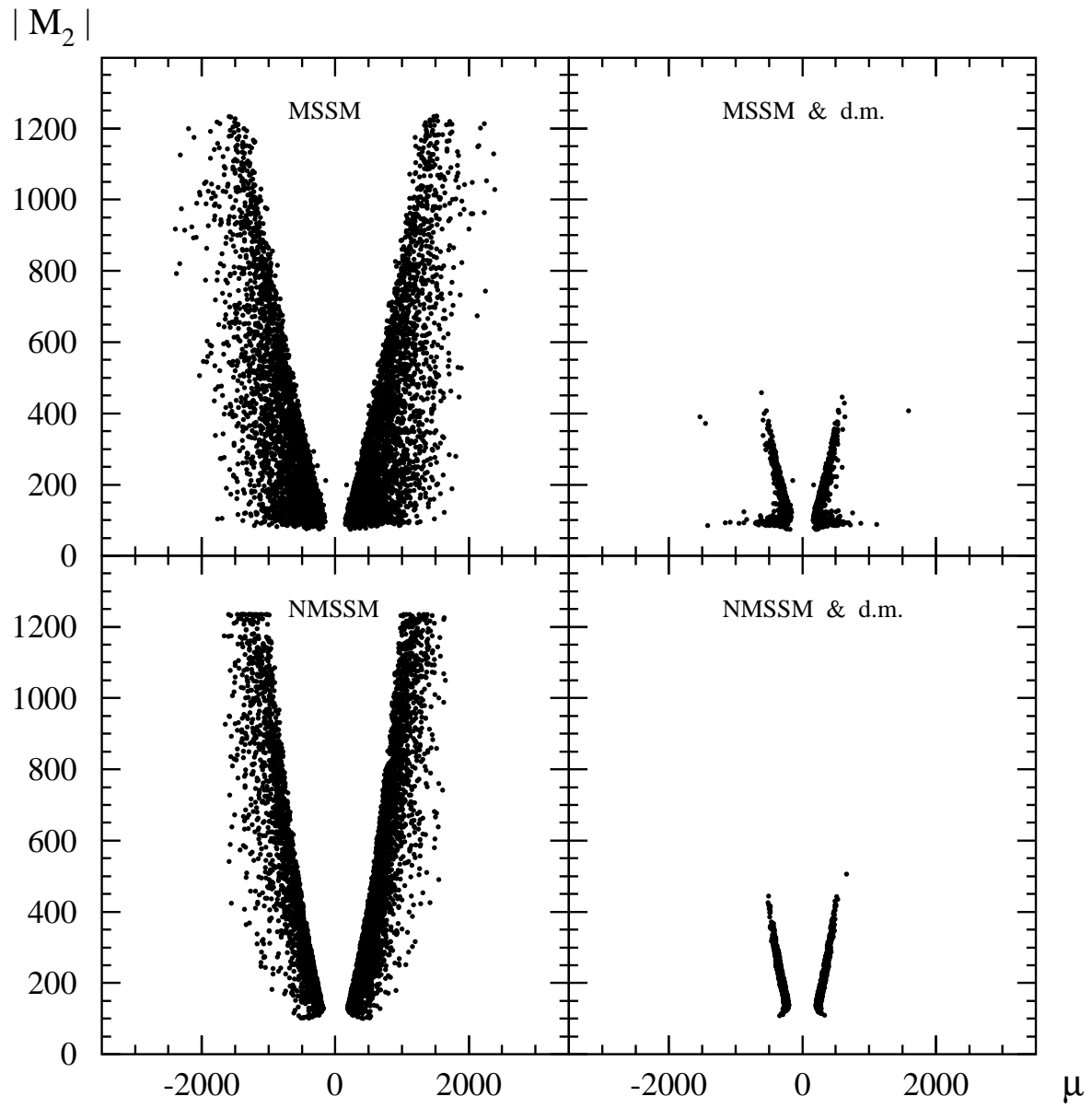


Fig. 3

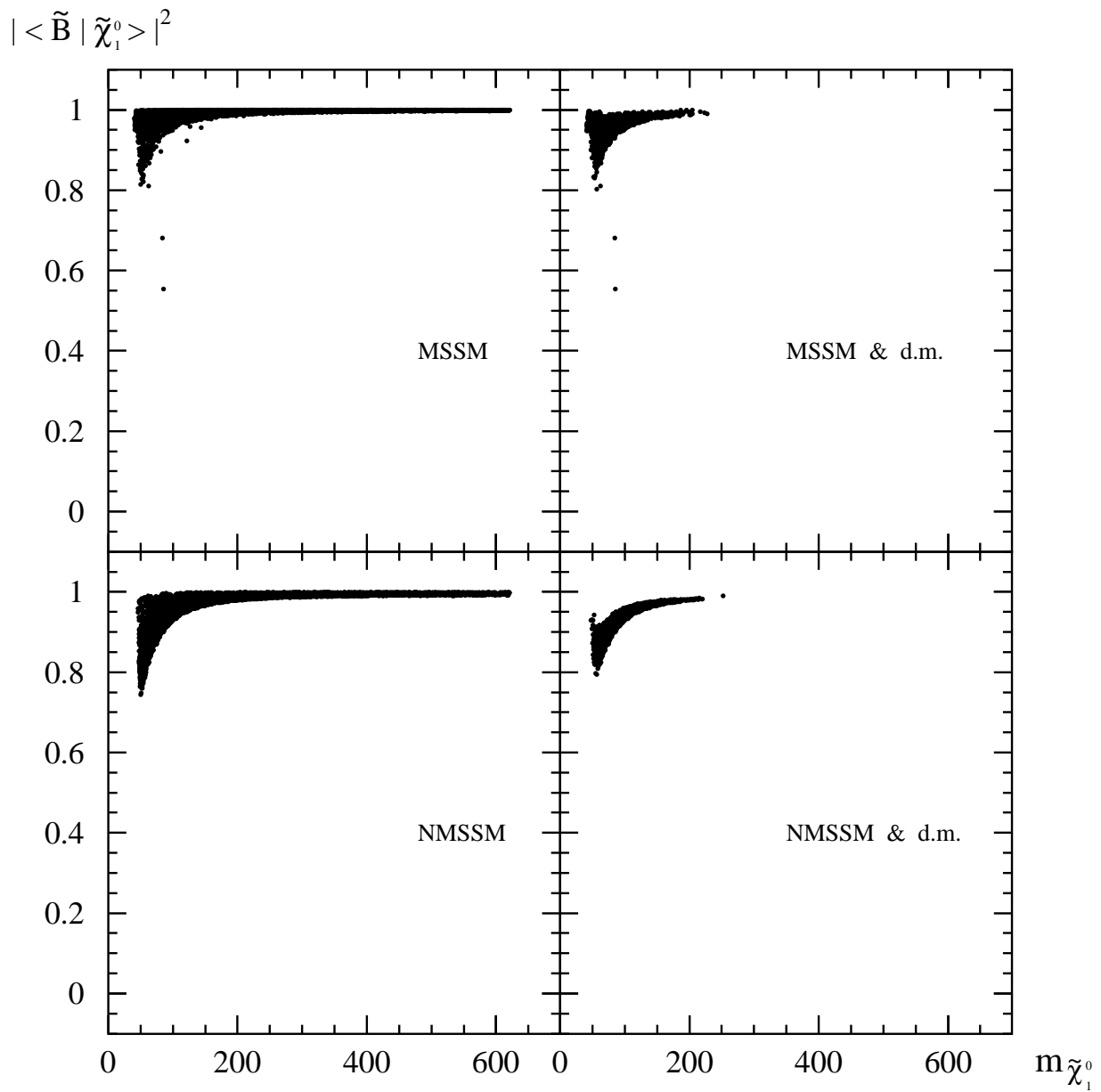


Fig. 4

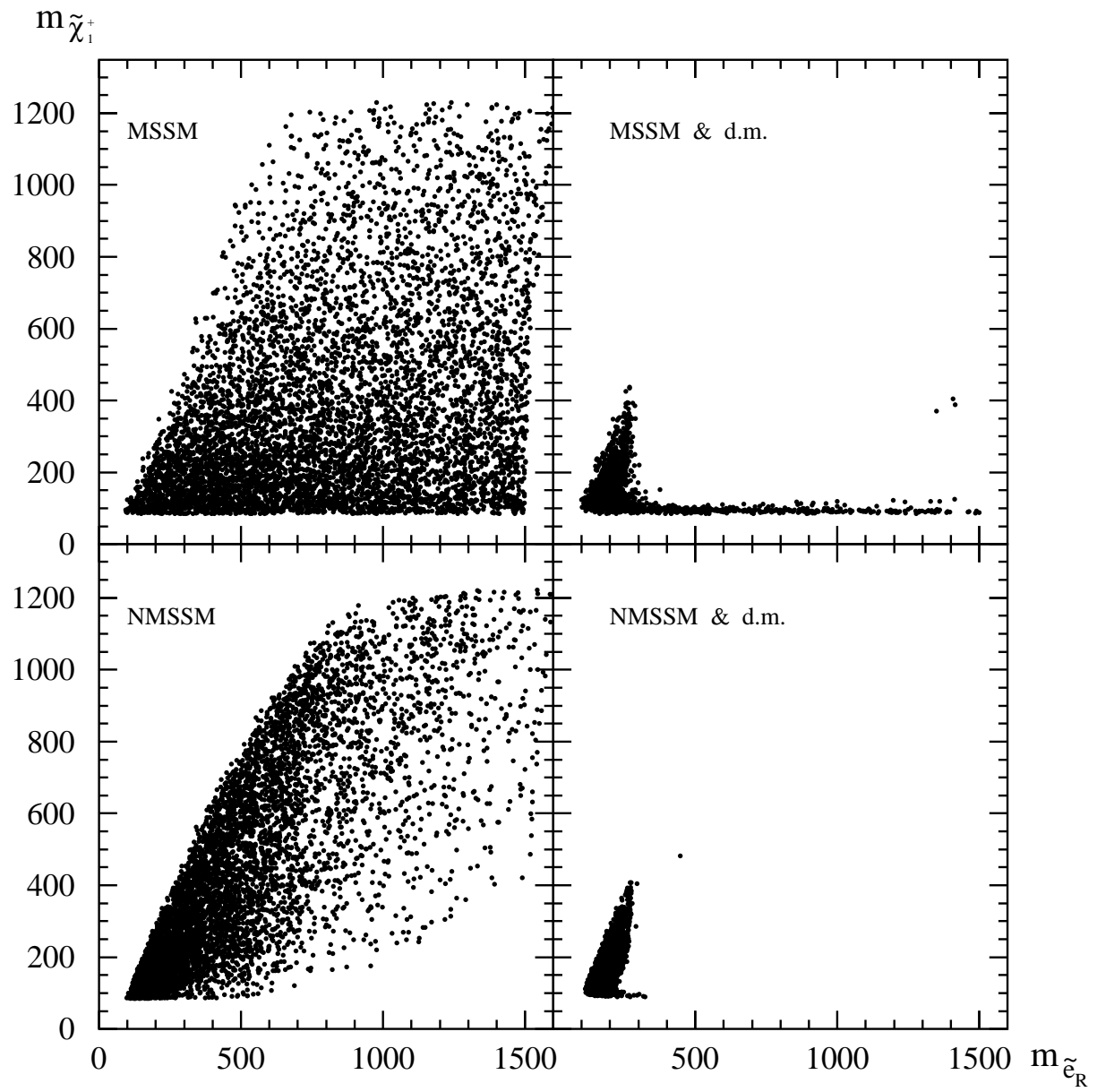


Fig. 5

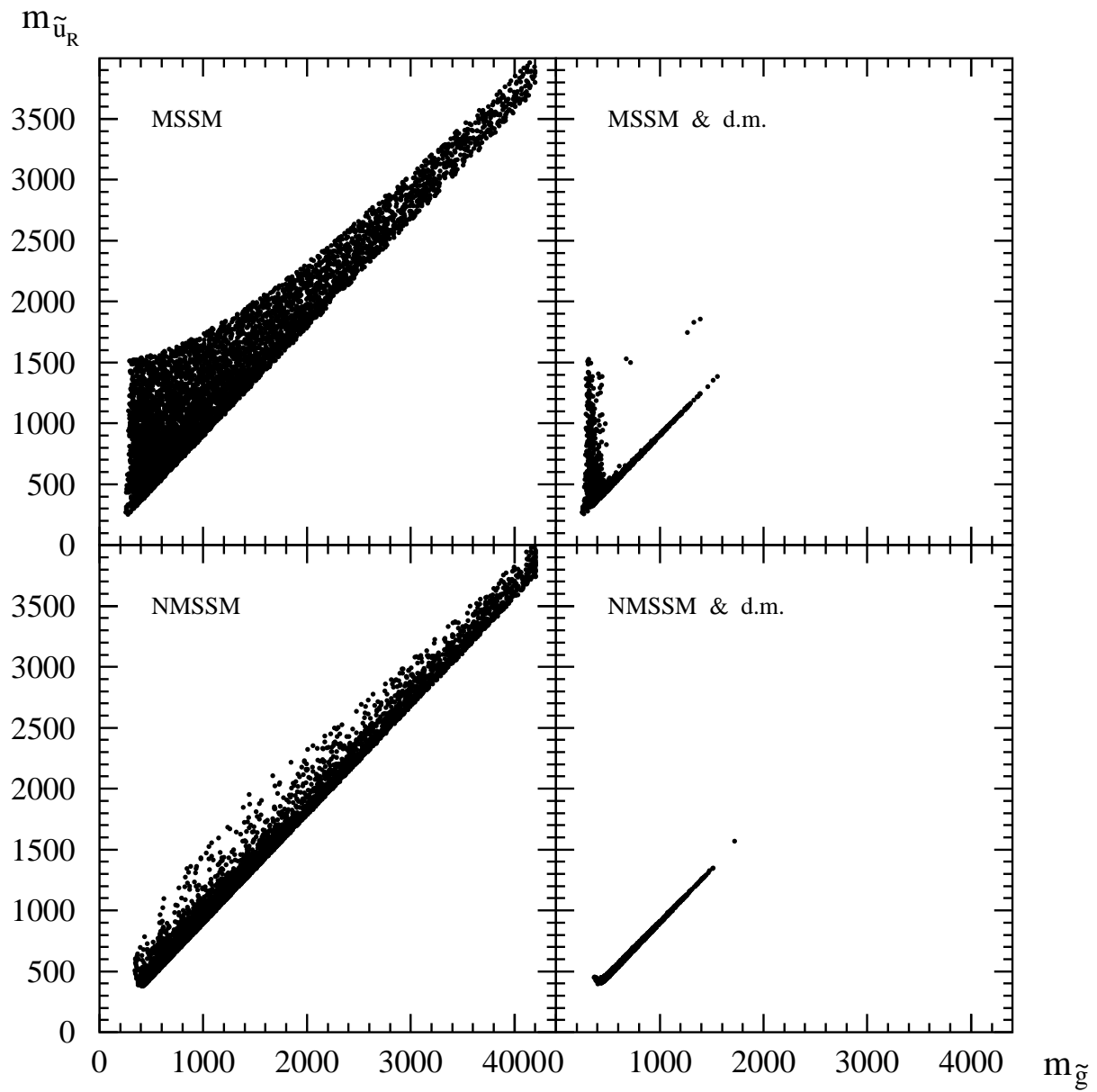


Fig. 6

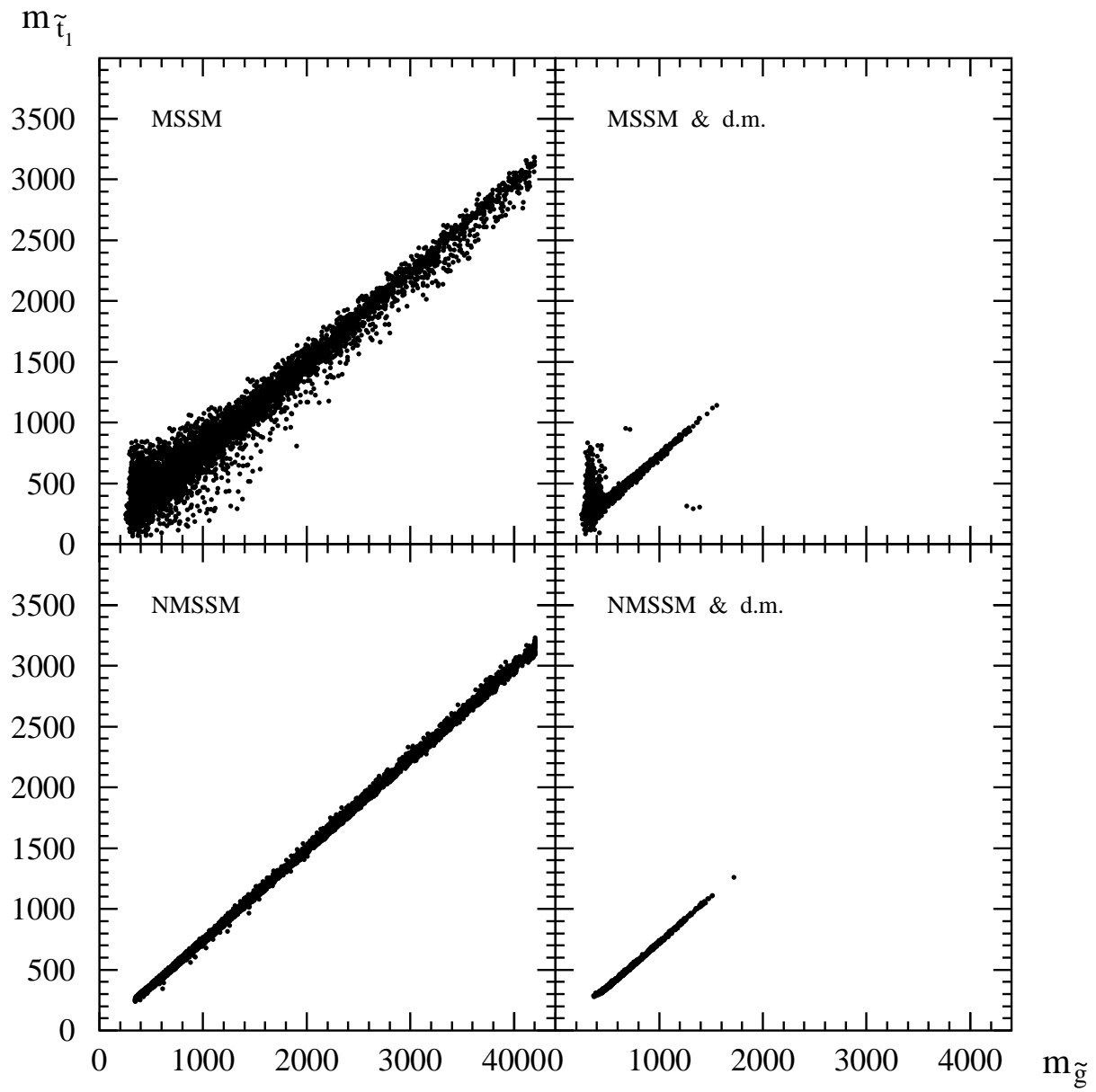


Fig. 7

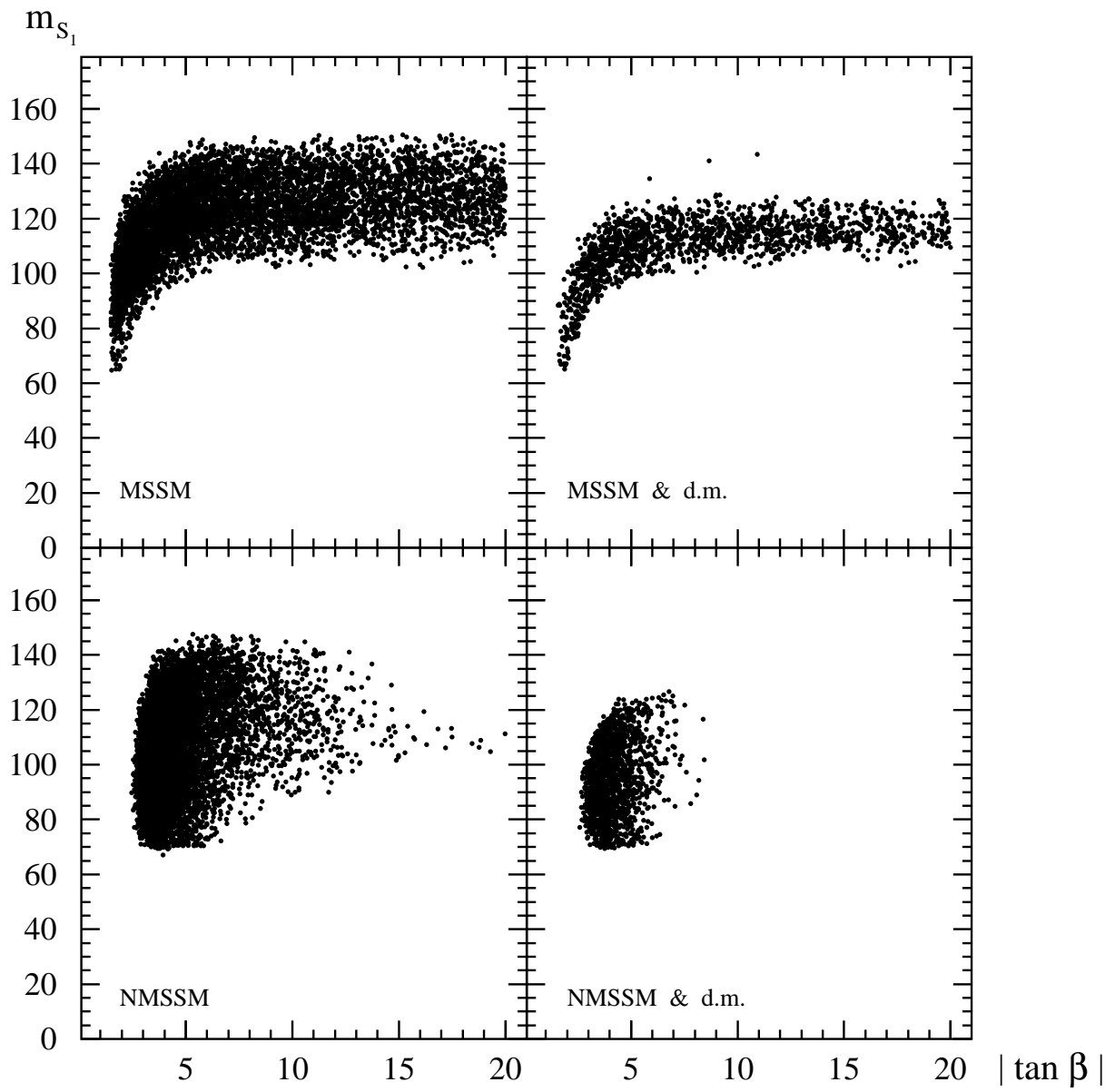


Fig. 8

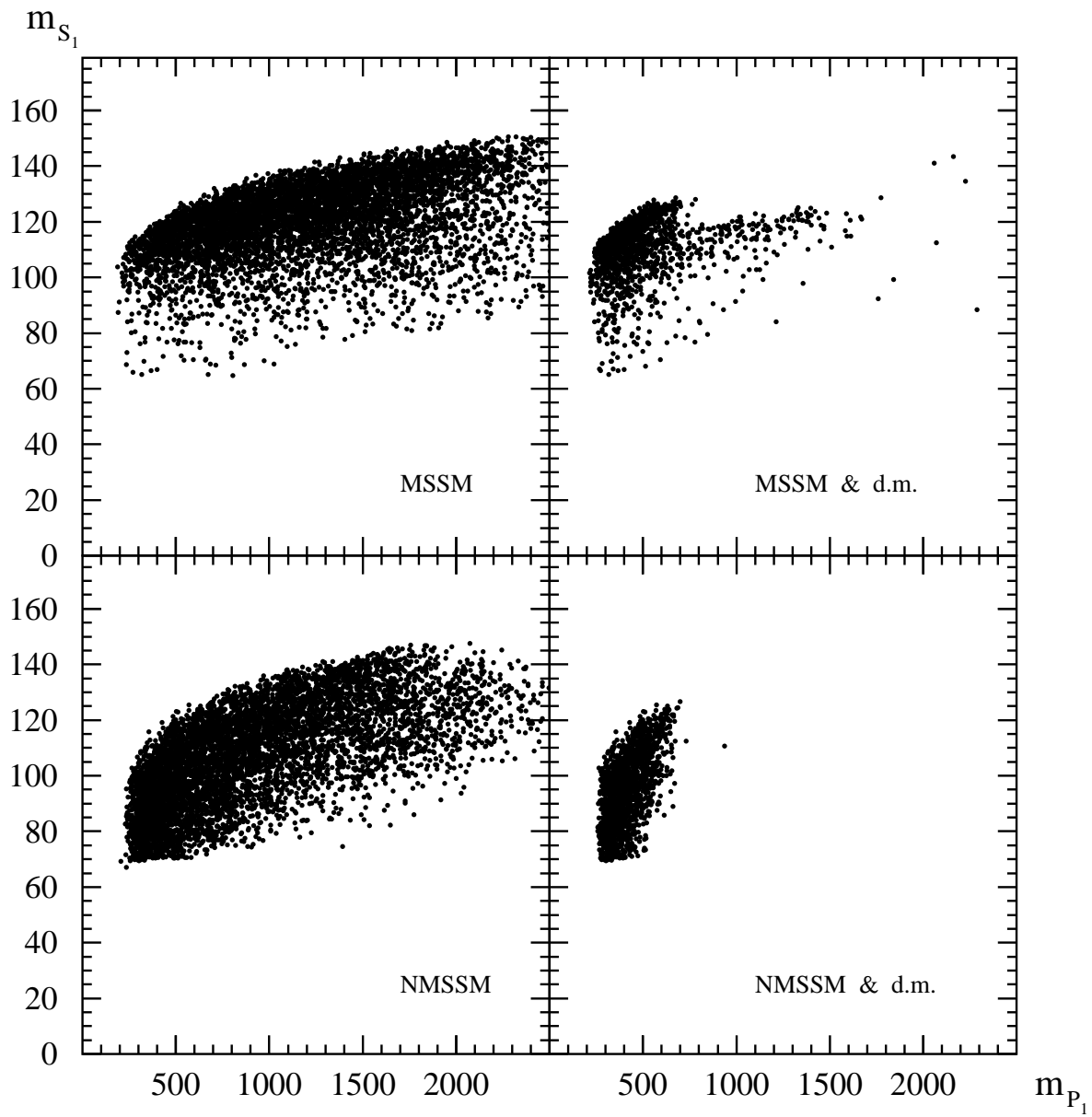


Fig. 9